Materials Horizons

ROYAL SOCIETY OF CHEMISTRY

REVIEW

View Article Online
View Journal | View Issue

Cite this: *Mater. Horiz.*, 2025, **12**, 3667

Memristive neuromorphic interfaces: integrating sensory modalities with artificial neural networks

Ji Eun Kim,†[ab] Keunho Soh,†[c] Su In Hwang,[c] Do Young Yang[c] and Jung Ho Yoon *[c]

The advent of the Internet of Things (IoT) has led to exponential growth in data generated from sensors, requiring efficient methods to process complex and unstructured external information. Unlike conventional von Neumann sensory systems with separate data collection and processing units, biological sensory systems integrate sensing, memory, and computing to process environmental information in real time with high efficiency. Memristive neuromorphic sensory systems using memristors as their basic components have emerged as promising alternatives to CMOS-based systems. Memristors can closely replicate the key characteristics of biological receptors, neurons, and synapses by integrating the threshold and adaptation properties of receptors, the action potential firing in neurons, and the synaptic plasticity of synapses. Furthermore, through careful engineering of their switching dynamics, the electrical properties of memristors can be tailored to emulate specific functions, while benefiting from high operational speed, low power consumption, and exceptional scalability. Consequently, their integration with high-performance sensors offers a promising pathway toward realizing fully integrated artificial sensory systems that can efficiently process and respond to diverse environmental stimuli in real time. In this review, we first introduce the fundamental principles of memristive neuromorphic technologies for artificial sensory systems, explaining how each component is structured and what functions it performs. We then discuss how these principles can be applied to replicate the four traditional senses, highlighting the underlying mechanisms and recent advances in mimicking biological sensory functions. Finally, we address the remaining challenges and provide prospects for the continued development of memristor-based artificial sensory systems.

Received 8th January 2025,
Accepted 5th March 2025

DOI: 10.1039/d5mh00038f

rsc.li/materials-horizons

Wider impact

The implementation of artificial sensory systems is essential for converting vast amounts of environmental information into input signals required for neuromorphic computing. When realized using memristors, such systems effectively compress signals during the conversion process while retaining adaptive, nociceptive, and spatiotemporal information critical for learning and inference. Furthermore, their compatibility with a wide range of sensors ensures excellent expandability, while the dynamic resistive switching properties of memristors enable the development of diverse signal conversion strategies. Memristor-based artificial sensory systems not only emulate human sensory processing but also offer significant advantages in terms of energy efficiency and miniaturization, making them highly suitable for edge computing and wearable technologies. Their ability to perform parallel signal processing can also enhance real-time decision-making in complex environments. Gaining insights into memristor-based artificial sensory systems, which process patterned sensory data akin to human perception, can drive future advancements in neuromorphic computing, industrial automation, and robotics.

1. Introduction

The growing demand for automation in supply chains, manufacturing, robotics, and unmanned vehicles has driven the development of artificial intelligence (AI) technologies. These technologies have the potential to significantly improve efficiency and autonomy across various industries using sensory systems comprising sensors and computational networks to sense the surroundings and acquire information from the environment in real time.[1,2] For instance, conventional complementary metal-oxide semiconductor (CMOS)-based systems have demonstrated intelligent recognition and control applications, such as image classification, natural language processing, and decision-making tasks.[3–10] However, because the von Neumann architecture physically separates memory and processing units,

[a] *Electronic Materials Research Center, Korea Institute of Science and Technology (KIST), Seoul 02791, Republic of Korea*
[b] *Department of Materials Science and Engineering, Korea University, Seoul 02841, Republic of Korea*
[c] *School of Advanced Materials and Engineering, Sungkyunkwan University (SKKU), Suwon 16419, Republic of Korea. E-mail: junghoyoon@skku.edu*
† These authors contributed equally to this work.

conventional systems require massive amounts of data transfer between them. This results in high power consumption and causes significant latency, commonly referred to as the von Neumann bottleneck, which fundamentally degrades the performance of AI applications.[11–14]

Unlike conventional systems, biological sensory systems detect, interpret, and store external information in a data-parallel and integrated manner.[15] This is enabled by receptors that generate electrical signals only when stimuli exceed a threshold, selectively adapting to harmless, repetitive inputs. These signals are transmitted as action potentials (spikes) through neurons to specific brain regions, where they are processed in an event-driven, adaptive, and parallel manner, enabling learning and inference.[16,17] Inspired by the energy-efficient and fault-tolerant nature of biological systems, neuromorphic computing has been developed to overcome the technical limitations of conventional CMOS-based systems.[18–21] It supports the integration, processing, and storage of sensory information, playing a crucial role in advanced functions, such as decision-making, cognition, learning, and memory. Moreover, neuromorphic computing can execute multiple tasks simultaneously in highly parallel settings with a low power consumption of 1–100 fJ per synaptic event.[22] The exceptional capabilities of memristors enable their integration with neuromorphic learning algorithms to facilitate advanced functions. Large-scale integration and hardware implementation using CMOS-compatible processes are essential to leverage these capabilities, with extensive research currently underway. The technology has now advanced beyond hybrid 1T1R structures, reaching a stage where fully memristor-based hardware implementations are feasible. This progress has demonstrated the practical applicability of memristors across various AI applications, validating their potential for widespread deployment.[23–27]

Therefore, it is crucial to implement artificial sensory systems capable of mimicking the roles of biological receptors, neurons, and synapses to fully leverage neuromorphic computing.[28–31] Although conventional CMOS-based electronics have been used to develop artificial synapses and neurons as neuromorphic devices, they are limited by circuit area and energy efficiency.[32–34] Since the CMOS-based devices are optimized for digital switching, they struggle to handle smooth and continuous signal variations, which are essential for accurately reflecting external stimuli. Thus, essential functions, such as the accumulation of external stimuli, the generation of corresponding output signals, and information storage, are inevitably performed by separate components. As a result, the emulation process compromises both area and energy efficiency in proportion to the number of devices used.[35] Moreover, implementing analog switching to achieve both the precision and dynamic range required for emulating biological counterparts remains a significant challenge in conventional CMOS-based systems. These systems necessitate the incorporation of additional circuitry, such as digital-to-analog converters (DACs), to facilitate analog switching. Although more complex DAC configurations are required to enhance the output resolution, the resulting output often lacks the desired smoothness. Meanwhile, among various neuromorphic devices, memristors stand out for their area-efficient structure as well as high-speed and low-power operation. Additionally, their excellent scalability, durability, and uniformity make them well-suited for the reliable implementation of artificial sensory systems.[36–40] Furthermore, a unique attribute of memristors is their ability to gradually switch between a low-resistance state (LRS) and a high-resistance state (HRS) in response to external stimuli, such as voltage or current. In other words, memristors exhibit continuous and dynamic resistive state changes rather than relying on binary resistance states. This enables the direct processing of analog external stimuli without the complex configuration of using multiple devices or peripheral circuits such as analog-to-digital converters. Therefore, the dynamic resistive switching provided by memristors is essential for replicating the artificial sensory systems, as they more efficiently capture the full fidelity of incoming signals. Owing to these advantages, memristors have been widely utilized in the implementation of artificial receptors, synapses, and neurons.[41,42] In particular, their material composition, device structure, and switching dynamics can be carefully engineered to optimize switching behavior, making them adaptable to both volatile and non-volatile properties—key characteristics for mimicking biological elements.[34,43–51] Thus, integrating memristive devices with various sensors facilitates the implementation of artificial sensory systems corresponding to tactile, visual, auditory, and olfactory modalities.[52,53]

In biological sensory systems, sensory receptors located in the sensory organs convert external perceptual signals into receptor potentials, and sensory neurons integrate these potentials to initiate action potentials. Finally, the synapses store the encoded sensory information. Similarly, in a bioinspired memristive sensory system, sensors generally convert external stimuli into electrical signals, which are then applied to memristors. Subsequently, the memristive receptor device that receives the signal generates a potential that is proportional to the input, incorporates information regarding harmful stimuli, and transfers it to the subsequent sensory system. Subsequently, the integrated memristive synapse and neural devices respond to input signals in a manner analogous to biological perception systems. By mimicking the biological sensory systems, the integration of sensory, processing, and memory components in bioinspired memristive systems enables high power efficiency, low latency, and excellent processing capabilities.

Despite the versatility of memristors, current research has predominantly focused on signal conversion based on their switching characteristics. This approach has contributed immensely to the advancement of neuromorphic computing by enabling reliable and direct conversion of external stimuli into signals that drive neural networks implemented in hardware and software. However, studies on how closely these conversions align with the behavior of the human nervous system are lacking. The existing memristor-based systems often fail to fully capture the intricate dynamics of biological sensory systems, particularly in terms of complexity and adaptability. Devices capable of replicating the full range of functions of biological receptors, neurons, and synapses remain exceedingly rare. Even at the individual level, most artificial systems struggle to replicate all the critical functions of a single biological element. In artificial sensory systems, this limitation is further compounded by the frequent exclusion of

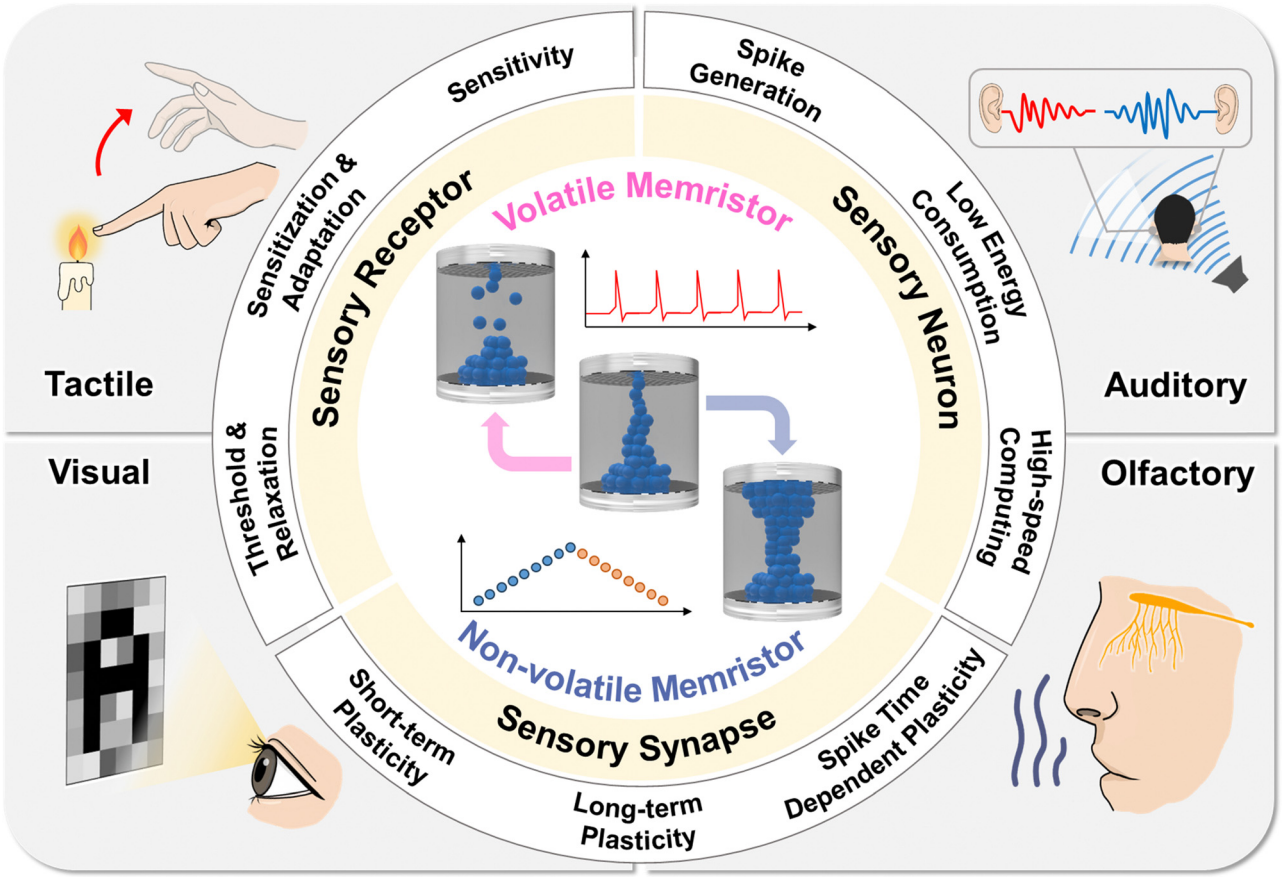

Fig. 1 Schematic of the artificial sensory system and functions, featuring integrated and collaborative networks of memristive receptors, neurons, and synapses.

specific functions or entire elements, resulting in incomplete or inefficient performance. This highlights a critical challenge: implementing all essential characteristics necessary for effective emulation. For artificial sensory systems to accurately process external stimuli across diverse environmental conditions, several crucial properties must be considered, including sensitivity, adaptability, and spatiotemporal processability. For instance, biological systems can dynamically adjust their sensitivity to external stimuli, such as by enhancing auditory perception in noisy environments or modulating visual processing under low light. Emulating this adaptability requires devices capable of self-tuning and learning in response to changing environmental conditions. Moreover, processing spatiotemporal patterns—similar to biological synapses responding to time-dependent signals—remains essential for replicating complex sensory functions. A systematic understanding of these properties is fundamental to developing artificial sensory systems that process complex input patterns with greater accuracy and efficiency.

In this review, the recent advances, challenges, and prospects of bio-inspired memristive artificial sensory systems are comprehensively examined. In this context, the switching performance metrics required for memristors in the implementation of artificial sensory systems, as depicted in Fig. 1, along with the sensory modalities they aim to emulate, are discussed. The subsequent sections first explore the fundamental roles of receptors, neurons, and synapses in biological sensory systems, along with the corresponding switching characteristics of memristors essential for replicating these neuronal components. Next, innovative cases of bio-inspired artificial sensory systems developed for the four primary senses—tactile, visual, auditory, and olfactory—are presented. Recent memristor research progress is then examined, focusing on how closely these systems mimic biological sensory functions and evaluating the effectiveness of these advancements. Finally, challenges and prospects for the development of memristor-based artificial sensory systems are addressed. This review aims to encourage ongoing research and development, fostering a deeper understanding and broader range of applications of bio-inspired sensory systems by analyzing the roles of receptors, neurons, and synapses, the switching dynamics of memristors, and the necessary characteristics for each type of neural implementation.

2. Elements of the nervous system: receptors, neurons, and synapses

To emulate the characteristics of receptors, neurons, and synapses using memristors, a comprehensive understanding of their operational mechanisms is required. Additionally,

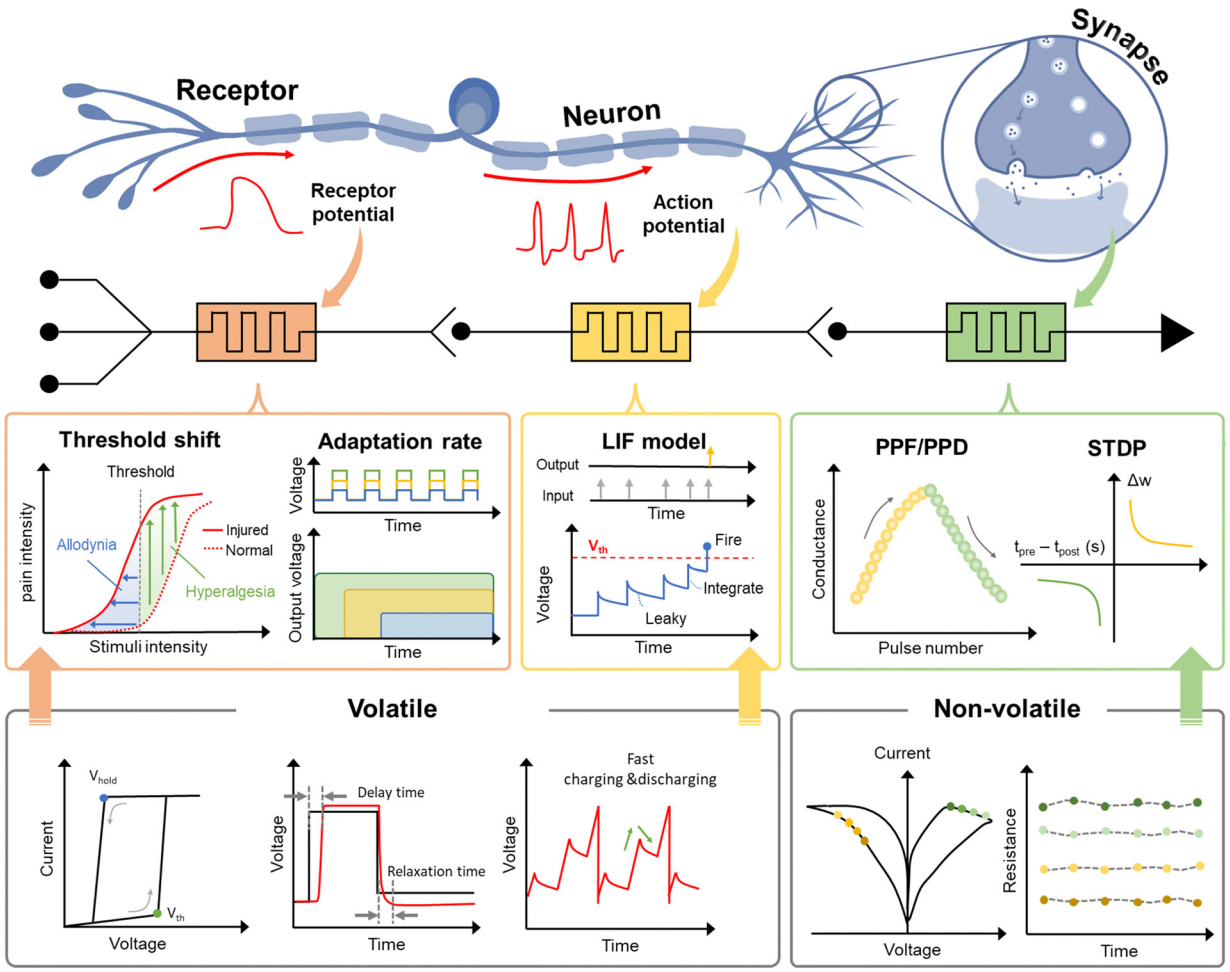

Fig. 2 Features and performances required to implement artificial sensory receptors, neurons, and synapses. Function characteristics of volatile and non-volatile memristors to mimic sensory elements.

investigating the switching properties of memristors and exploring how these properties can be utilized to mimic each component are essential. This process is crucial for precisely controlling the electrical characteristics of memristors and effectively reproducing the complex functions of the nervous system, as shown in Fig. 2.

2.1. Receptors

Receptors play a crucial role in detecting and responding to various stimuli, enabling us to perceive and interact with the environment.[54,55] Receptors convert physical and chemical stimuli into electrical signals. This process enables humans to appropriately respond to stimuli. Receptors have evolved to be specifically responsive to stimuli and can be classified into categories based on their ability to accommodate different external stimuli, such as mechanoreceptors, thermoreceptors, photoreceptors, chemoreceptors, and nociceptors.

Receptors operate based on thresholds and relaxation.[56] The threshold indicates the minimum intensity of a stimulus required to be activated, below which the receptor remains unresponsive. This characteristic enables the receptors to filter out insignificant minor stimuli and focus on more critical signals. Upon activation by external stimuli, receptors transition into a relaxed state where their responsiveness to the stimulus gradually diminishes, enabling them to revert to their initial state. During the relaxation state, receptors retain a certain degree of activation; consequently, the threshold intensity of the stimulus for reactivation is reduced compared with that of the initial activation. This phenomenon, known as sensitization, is crucial for modulating receptor sensitivity.[57] Additionally, some receptors exhibit adaptation characteristics, whereby their response diminishes in the presence of continuous stimuli. These receptors provide essential protection against persistent and harmful stimuli while also preventing energy expenditure on non-essential stimuli.

The volatile memristor is suitable as an artificial nociceptor because it reacts only to electric pulses above a certain threshold and gradually reduces the output signal once the pulse is removed.[58–60] Moreover, such threshold and relaxation behaviors strongly depend on the strength, period, and duration of the input signal. Regulating relaxation enables the mimicry of phenomena observed in certain receptors, such as allodynia, in which the threshold is lowered upon exposure to harmful stimuli, and hyperalgesia, in which the response is amplified.

In addition, this approach enables the implementation of adaptation functionality, which allows the receptors to adjust to repeated stimuli. The detailed mechanisms and applications are discussed in Section 3.

2.2. Neurons

Neurons constitute the fundamental units of the nervous system that transmit electrical signals generated by external stimuli at receptors in the brain, enabling recognition and response to these stimuli.[61,62] Neurons are primarily composed of the cell body (soma), dendrites, and axons. The soma acts as the metabolic and genetic center of the neuron, housing the cell nucleus and supporting vital cellular functions. Dendrites extending from the soma receive signals from other neurons or sensory receptors, whereas axons transmit electrical signals to other neurons and muscles. These electrical signals are generated from rapid changes in the membrane potential of the axon, known as the action potential.[63] When the action potential reaches the axon terminal, neurotransmitters are released into the synapse and subsequently interact with the dendrites of the postsynaptic neuron. Synaptic transmission facilitates the formation of complex neural networks that enable information collection, integration, transmission, and coordination. Neurons are classified based on their functions and characteristics. For instance, sensory neurons detect external stimuli, such as light, sound, and temperature, and transmit this information to the central nervous system. Motor neurons carry commands from the central nervous system to the muscles or glands. Interneurons function as intermediaries, processing and relaying information between sensory and motor neurons.

Volatile memristors are well-suited as artificial neurons due to their ability to exhibit a steep current response exceeding a threshold stimulus, followed by a decrease through volatile switching—closely mimicking action potentials. Additionally, they effectively integrate inputs from multiple channels and generate repetitive spike signals with frequencies proportional to the combined input levels. During signal generation, volatile memristors dynamically adjust their responses based on input strength and frequency, efficiently encoding continuous analog signals into spike trains—similar to biological neurons. This adaptability enables differentiation between weak and strong stimuli, replicating sensory adaptation mechanisms in the human nervous system. Recent studies have demonstrated the implementation of Hodgkin–Huxley (HH) and leaky integrate-and-fire (LIF) model neurons using volatile memristors, further highlighting their compatibility with biological neuron models. These models leverage the ability of memristors to replicate essential neuronal behaviors such as voltage-dependent conductance and firing dynamics. Specifically, artificial neurons constructed using volatile memristors encode temporal information by adjusting their spiking frequency based on the input intensity, closely resembling the time-dependent stimulus information of biological sensory neurons. Moreover, memristor-based implementations offer advantages such as low power consumption and scalability while achieving comparable performance to biological neurons.

2.3. Synapses

Synapses serve as junctions between the axon of one neuron and the dendrite of another, playing an essential role in neural transmission.[52,64] When an electrical signal reaches the axon of a presynaptic neuron, the synapse adjusts the connection strength (synaptic weight) based on the input signal, either strengthening or weakening the synaptic weight. The dynamic regulation of synaptic weight is fundamental to learning and memory and serves as a critical component in understanding the functional mechanisms of the human brain. Adjustments in synaptic weight, such as spike-timing-dependent plasticity (STDP), short-term plasticity (STP), and long-term plasticity (LTP), are fundamental to the ability of the brain to adapt, learn, and form memories.[65–67] STDP is used to effectively control synaptic weight, demonstrating a type of synaptic plasticity that depends on the exact timing between the two neurons. This mechanism facilitates the efficient utilization of neural networks by leveraging the temporal interactions between neurons. STP refers to temporary changes in synaptic strength. The STP lasts from a few seconds to several minutes and can fluctuate based on the activity patterns of the neurons. It is primarily governed by intracellular mechanisms associated with neurotransmitter release and plays a crucial role in adapting to rapidly changing environments and processing transient information. Unlike STP, LTP is required for long-term memory formation. LTP refers to the sustained enhancement of synaptic strength over extended periods, ranging from hours to years. It is known to play a critical role in learning and memory processes and arises from the repeated activation of specific neural paths.

Non-volatile memristors are highly suitable for mimicking synaptic characteristics.[59,68,69] Non-volatile memristors exhibit resistance changes in response to electrical stimuli, effectively replicating the synaptic weight. Furthermore, the switching behavior of non-volatile memristors, which allows them to retain information even in the absence of a bias, enables the emulation of long-term memory functionality. The modulation of resistance and synaptic weight assumes a critical function for assessing the intensity of previous input signals within the frameworks of machine learning and neural network algorithms. The linearity of resistance modulation is crucial and can be effectively utilized to deduce the strength of the signals. Linearity is essential for improving the precision of the numerous algorithms used in machine learning and neural networks. Furthermore, the potential of utilizing non-volatile memristors to emulate the characteristics of synaptic devices has been demonstrated, enabling the replication of various forms of synaptic plasticity such as LTP, STP, and STDP. In detail, non-volatile memristors can exhibit STDP behavior, where synaptic strength is modified based on the timing of pre- and post-synaptic input spikes. In addition, LTP and STP can be achieved by adjusting the device conductance in response to varying input frequencies, allowing non-volatile memristors to adapt to both transient and sustained input patterns. This is achieved through the precise control of the formation of conductive pathways, which are closely associated with resistance changes in non-volatile memristors. This approach can effectively reproduce the dynamic properties of

synaptic plasticity. These findings demonstrate the ability to implement various forms of synaptic plasticity and memory functions, highlighting their potential suitability for efficient brain-inspired computing architectures.

3. Memristor-based tactile sensory systems

Human skin enables us to recognize objects and interpret the environment through the sense of touch. Tactile perception is complex and involves sensing, refining, learning, and forming interactions with the external environment.[70–73] Receptors on sensory neurons embedded in the skin, such as nociceptors, chemoreceptors, and mechanoreceptors, detect various somatic sensations and convey tactile information to the brain *via* electrical signals. This process enables exquisite sensations of object recognition, texture discrimination, and sensory feedback. Tactile receptors can detect even small amounts of pressure or force, and when combined with external stimuli, they provide a detailed and nuanced picture of the object or surface being touched. This information can help humans navigate their environment, manipulate objects, and perform tasks that require a sense of touch. They can also improve the functionality and comfort of prosthetic limbs by providing users with a more natural and intuitive sense of touch. This chapter explains memristor-based electronic tactile sensory systems related to somatic sensations.

3.1. Memristor-based nociceptors and adaptive receptors

Nociceptors play a vital role in mimicking human acceptance and processing of external stimuli. When a stimulus such as mechanical stress, chemical stress, or temperature is applied, the nociceptor determines the degree of hazard and generates the corresponding biochemical signals. Therefore, to assess the danger posed by external stimuli and to respond to and safeguard oneself, all diverse features must be incorporated into the nociceptor.[74,75]

Memristor-based nociceptors are similar to bionociceptors in that they respond differently to different stimuli. As shown in Fig. 3a, Yoon *et al.* established an artificial nociceptor based on an Ag-based threshold-switching memristor with the function of a nociceptor that implements four key functions (threshold, relaxation, no adaptation, and sensitization).[76] Allodynia and hyperalgesia, resulting from harmful or abnormal stimuli, can be effectively induced in memristors by applying high voltages that exceed the threshold level. When the input voltage is increased to a level perceived as harmful, the conductive paths in the memristor grow excessively, making spontaneous and complete rupture challenging after the voltage is removed. Consequently, residual Ag clusters or conductive paths remain within the oxide film, facilitating a rapid response to stimuli below the threshold (sensitization). To further demonstrate the potential of the nociceptor, an artificial Ag-based nociceptor memristor was integrated into the thermoelectric module. The thermal nociceptor only generated an electric spike at a critical temperature (50 °C, hazardous temperature). As the temperature increased, the signal amplitude increased, and the onset time decreased.

Kim *et al.*[79] reported an artificial nociceptor based on a Pt/HfO_2/TiN memristor utilizing trap/detrap mechanisms instead of a cation-based threshold-switching memristor. The nociceptive function was imitated by adjusting the trap depth of the HfO_2 layer. When a sufficiently high positive voltage was applied to Pt, lowering the trap level below the Fermi energy level of TiN facilitated electron injection from TiN to fill the trap sites. Once filled, the electron transport increased sharply due to trap-assisted tunneling conduction between trap sites, turning the device on (threshold switching). After the voltage was removed, the difference in work functions between the Pt and TiN electrodes created a built-in potential that caused the trapped electrons to relax over time (relaxation). The device exhibited a wide operation time span ranging from milliseconds to ten seconds, with a relaxation time scale well-matched to typical biological systems making it highly effective for mimicking nociceptor behavior. Therefore, additional circuits have been designed to effectively mimic biological reflex actions, enabling immediate response generation and transmission to the spinal cord when exposed to danger.

There is an increasing need for humanoid robots to imitate advanced biological functions to respond efficiently to external environments. Biological skin can protect itself against harmful damage by detecting the degree of danger and initiating appropriate actions using nociceptors. Moreover, biological skin can self-heal and eventually return to its normal state when damaged by external stimuli. The design of a memristor is crucial for mimicking the complex characteristics of bioskin. Xiaojie *et al.* reported an artificial sensory system with the ability to sense and warn patients of pain and heal itself. The FK-800-based organic volatile memristor acted as an electronic skin (Fig. 3b).[77] Self-healing was achieved because of the intrinsic characteristics of the organic material, similar to human skin. In addition, to sense pain and signs of injury, the artificial tactile system was composed of a triboelectric generator, volatile memristor, and light-emitting diode (LED). The triboelectric generator and volatile switching memristor act as mechanoreceptors and nociceptors, respectively. The triboelectric generator generates an output voltage based on the intensity of the external stimulus, and the generated voltage is applied to a volatile memristor. When a voltage above the threshold value was applied to the volatile memristor, the memristor and LED turned on. This case was considered to have minimal damage or pain and was not considered a threat. When a voltage below the threshold value was applied, the memristor and LED did not turn on, causing no damage or pain. Conversely, when a large input voltage was applied to the memristor as a strong stimulus, the relaxation time and resistance of the volatile memristor were longer and lower, respectively. Therefore, the LED was stronger and required a longer time to turn off completely.

To effectively perceive the external environment, it is essential to recognize both harmful and incoming nonharmful stimuli. Nociceptors react to potentially harmful stimuli such as pressure, heat, or chemicals, transmitting signals to the brain, where they are interpreted as pain. They respond consistently to

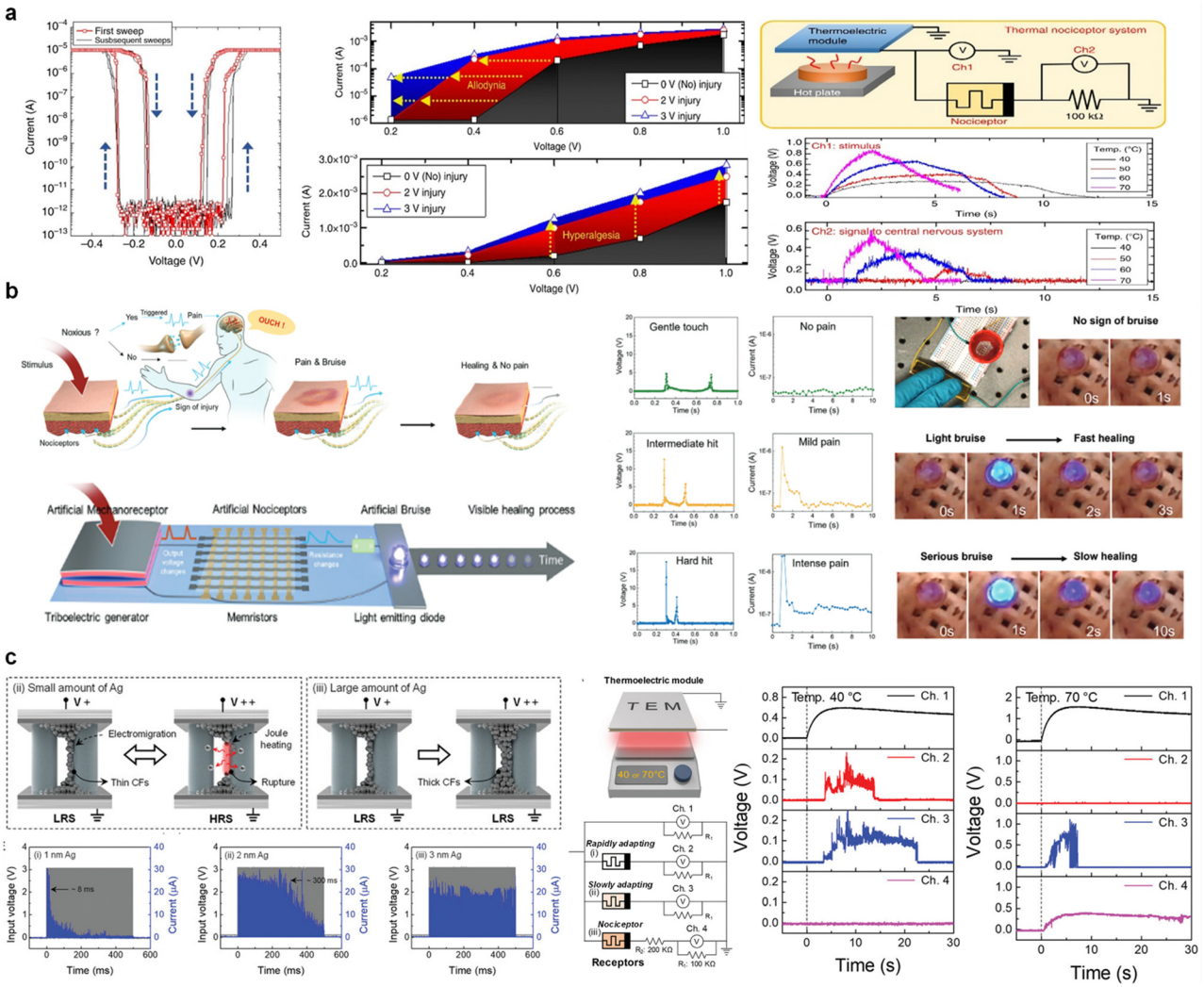

Fig. 3 (a) Threshold switching behavior, allodynia, and hyperalgesia. Schematic of an artificial thermal nociceptor circuit comprising a thermoelectric module and a volatile memristor. Generated voltage by a thermoelectric module and threshold switching behavior. Reproduced with permission from ref. 76. Copyright 2018 Springer Nature. (b) Bio-inspired artificial injury response system including a sense of pain, sign of injury, and healing. Lighting of light-emitting diodes (LEDs) according to intensity of stimulation. Reproduced with permission from ref. 77. Copyright 2022 John Wiley and Sons. (c) Pulse response of memristors to multiple 100 μs pulse widths with an amplitude of 3 V. Adaptation rates of 1, 2, and 3 nm Ag memristors are classified as rapidly, slowly, and no-adapting, respectively. Circuit schematic of an artificial sensory nervous system. Generated voltage from the thermoelectric module and volatile memristors was monitored by oscilloscope channels at hot plate temperatures of 40 and 70 °C. Reproduced with permission from ref. 78. Copyright 2021 John Wiley and Sons.

specific types of stimuli (no adaptation). In contrast, adaptive receptors reduce their sensitivity when exposed to continuous stimulation (adaptation), facilitating the filtration of unimportant and repetitive information.[80,81] This mechanism is essential for sensory processes such as vision, hearing, and touch, allowing humans to adjust to dynamic surroundings.

However, its implementation is difficult for both the existing CMOS-based and memristor-based receptors. Song *et al.* proposed an artificial receptor that mimicked both the adaptive and maladaptive characteristics using an Ag-based volatile memristor.[78] The artificial receptor was implemented by adjusting the thickness of the conductive filament with varying amounts of metal ions. The competitive relationship between Joule heating and electromigration was controlled by the number of metal ions, which determined the thickness of the conductive filament. Fig. 3c shows that the thin conductive filament (low Ag concentration) ruptured due to Joule heating during high-intensity stimuli (adaptive receptor), whereas the thick filament (high Ag concentration) maintained an electrical on-state (maladaptive receptor). Thus, the authors demonstrated the feasibility of implementing normal sensory-receptor behaviors.

3.2. Tactile stimulus perception

Artificial electronic skin, which captures surrounding tactile stimuli, is deployed in advanced intelligent systems. Conventionally, artificial electronic skin requires additional external equipment to store and process large amounts of data. However, this structure is inefficient in terms of energy

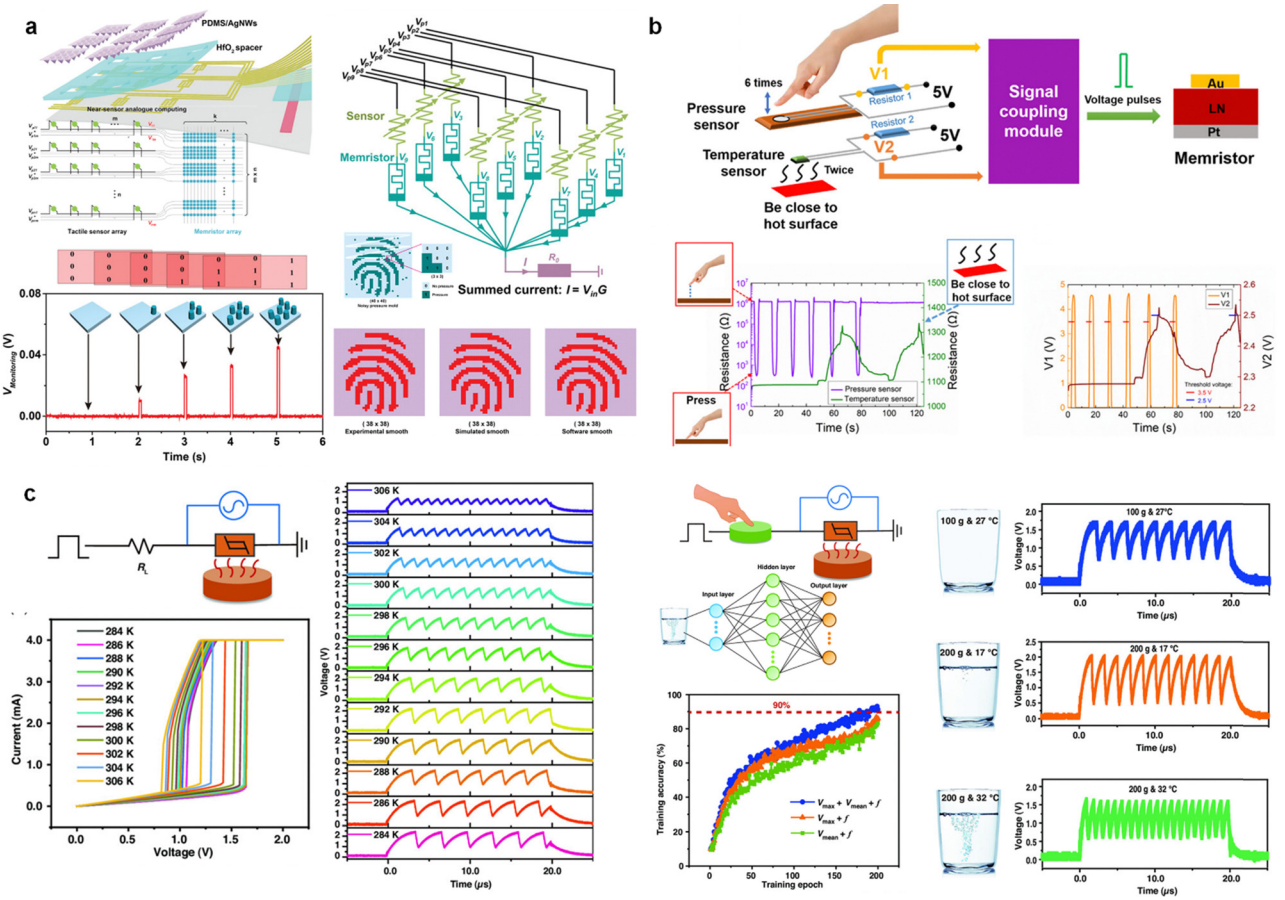

Fig. 4 (a) Near-sensor analog computing using an artificial tactile system. Resistance changes in a synapse memristor using a continuous pulse train. Near-sensor analog computing for real-time edge detection of the captured pressure pattern. Reproduced with permission from ref. 85. Copyright 2022 John Wiley and Sons. (b) Multimodal sensory system with multi-sensors accepting pressure and temperature stimuli. Resistance modulation of the pressure and temperature sensors as a response to pressure and hot stimuli. Reproduced with permission from ref. 86. Copyright 2022 John Wiley and Sons. (c) Characterization of an artificial temperature perception VO_2-based neuron memristor. Haptic-temperature fusion is based on a VO_2 volatile memristor and MLP by simulation. Reproduced with permission from ref. 87. Copyright 2022 John Wiley and Sons.

consumption and processing speed because it causes time delays and large energy consumption. Memristor-based tactile sensory systems can effectively emulate the functions of human tactile nerves in low-power operations without requiring additional equipment. Memristor-based tactile sensory systems enable the recording of stimuli by translating external mechanical stimuli into modulated electrical spikes. To mimic a tactile sensory system, an artificial system generally comprises a bio-inspired synaptic or neuron memristor and various sensors for detecting the external environment. The sensor connected to the memristor detected the strength of the external stimulus and generated various electrical signals based on the degree of stimulation applied. The memristor integrates the output signals of the parallel sensor and processes them into unified electrical spikes.[82–84]

Wang *et al.*[85] demonstrated an ultrafast artificial skin system based on near-sensor analog computing architecture. The artificial skin was implemented by combining a memristor with a tactile sensor and was fabricated on a flexible substrate. When a tactile sensor recognizes an external stimulus, an input pulse is generated and applied to the memristor to alter its resistance. Accordingly, the system simultaneously captures and processes the tactile stimuli in real time. In addition, the authors suggested that the system could be mounted on a finger or prosthesis to detect the edge information of external objects in real-time (Fig. 4a).

Sensory systems can simultaneously receive and transmit various types of information from the environment *via* various receptors. Similar to human reliance on multiple stimuli for decision-making and responses, artificial nervous systems that utilize memristors require the integration of information from diverse external stimuli to achieve effective functionality. Artificial sensory systems aim to achieve multisensory functions by simultaneously integrating and processing various sensory input signals. The first approach involves integrating the input signals obtained from a circuit comprising multiple sensors and a memristor. Xinqiang *et al.*[86] developed a multimodal sensory system that utilized pressure and temperature sensors in conjunction with non-volatile memristors and employed a signal coupling method to integrate the outputs (Fig. 4b). The input stimulus can be integrated from different sensors, and an output signal can be generated once the input signal from each sensor

reaches a fixed threshold voltage. Six pressed and two hot stimuli were applied to the system, which recognized eight stimuli and generated an eight-fold output. Correspondingly, the memristor reacted to several toxic stimuli and modulated conductance. This study demonstrates that a multimodal artificial sensory system can be constructed using different sensors (pressure and temperature) and signal-coupling modules.

A multimodal sensory system can be realized using memristor materials. This approach simplifies the circuits that constitute the multimodal sensing, making it efficient and advantageous in terms of energy utilization. Qingxi *et al.* developed a multisensory system by configuring an oscillation circuit using piezoresistive sensors and a VO_2-based volatile memristor (Fig. 4c).[87] VO_2 exhibits inherent thermal sensitivity, which enables its resistance state and characteristics to change in response to temperature fluctuations. Consequently, the VO_2-based memristor enables the monitoring of temperature stimuli without the need for supplementary sensors. When direct thermal stimuli are applied to a memristor, the inherent thermal sensitivity characteristics of VO_2 alter the switching behavior, thereby inducing a change in the oscillation circuit characteristics. In addition, when haptic actions are applied to a piezoresistive sensor, the magnitude of the stimulus alters the output of the sensor, which in turn changes the voltage applied to the non-volatile memristor, consequently modifying the oscillation characteristics of the volatile memristor. Therefore, without multiple sensors or electrical modules, an artificial mechanical sensory system can effectively synchronize information regarding external stimuli through vibrations that vary in response to pressure and temperature.

Memristor-based tactile receptors effectively detect various external stimuli, including heat and pressure. These receptors mimic the ability to recognize external stimulus patterns and generate appropriate responses through sensor integration and computational analyses. However, integration of sensors remains energy inefficient, and research on their ability to process multiple stimuli simultaneously remains limited. Further investigation is needed on software-based approaches for classifying and analyzing simultaneous stimuli, such as applying algorithms similar to the single-coupling module shown in Fig. 4b. These additional approaches can enhance the accuracy of human tactile system emulation.

4. Memristor-based visual sensory systems

Human vision is the primary method used to assess the size, shape, color, brightness, distance, and surface roughness of an object. Humans acquire more than 80% of their external information through the visual sensory system. In the information acquisition process, the eyes, brain, and muscles collaborate to perceive light stimuli and protect oneself by responding to potentially harmful stimuli.[88–90] The human visual sensory system rapidly processes these complicated tasks in a highly accurate and energy-efficient manner. Thus, mimicking this system is desirable for the efficient detection, processing, and storage of large volumes of visual information. However, the biological visual system features a complex hierarchical organization, including neural structures, such as the retina, bipolar cells, horizontal cells, and ganglion cells. Consequently, mimicking this system by using electronic circuits requires highly complex circuits and substantial energy consumption for information processing. Therefore, the development of more compact and efficient artificial visual sensory systems that can integrate sensing, processing, and storage functions is required. In this section, we describe a method that mimics human visual characteristics, such as light and motion detection, and the perception of an object using a memristor. This approach employs a memristor to mimic the visual adaptation functions, enhance efficiency, and reduce the complexity of an artificial visual system.

4.1. Retina-like preprocessing

The retina contains photoreceptors that detect external stimuli and transmit visual data to bipolar cells, which serve as intermediaries between the photoreceptors and ganglion cells. The data are then relayed through synapses with ganglion cells, triggering action potentials that travel to the lateral geniculate nucleus (LGN). The LGN transmits these signals to the visual cortex. In this process flow, a memristor can process information related to light intensity, directly detect the light intensity, or appropriately adapt to changes in the ambient light levels of the external environment.[91,92]

Dang *et al.*[93] demonstrated that the one-phototransistor–one-memristor (1PT1R) synaptic device shown in Fig. 5a has the potential for in-sensor computing and edge computing in visual sensory systems. In the 1PT1R structure, the ZnO-based phototransistor provides a driving current proportional to the light illumination, enabling the implementation of a high-linearity light-tunable multilevel conductance state within the $Mo/SiO_2/W$ memristor. Moreover, an optical artificial neural network (OANN) composed of a 16×3 1PT1R array performs cross-talk-free conductance updates because the phototransistor functions as a selector. The proposed OANN achieved a 99.3% accuracy in image recognition, demonstrating that the 1PT1R device is a promising hardware solution for artificial visual systems.

Shan *et al.*[94] demonstrated fully light-modulated synaptic plasticity using a plasmonic optoelectronic memristor comprising Ag nanoparticles embedded in a TiO_2 nanoporous film. Fig. 5b illustrates the photooxidation and reduction processes of the Ag nanoparticles embedded in the device under UV/vis irradiation. Under visible light irradiation, electrons from Ag transferred to the conduction band of the TiO_2 film, generating Ag^+ ions. This increased the effective diameter of the Ag conducting filament, thereby enhancing device conductivity. In contrast, UV irradiation excited electrons in the valence band of the TiO_2 film to its conduction band, which reduced the number of Ag^+ ions and suppressed the increase in device conductivity. Consequently, when electrical pulses were applied after UV and visible-light irradiation, the current response was greatly improved only under visible-light irradiation. This enables the emulation of light-induced and gated synaptic plasticity. The STDP learning was

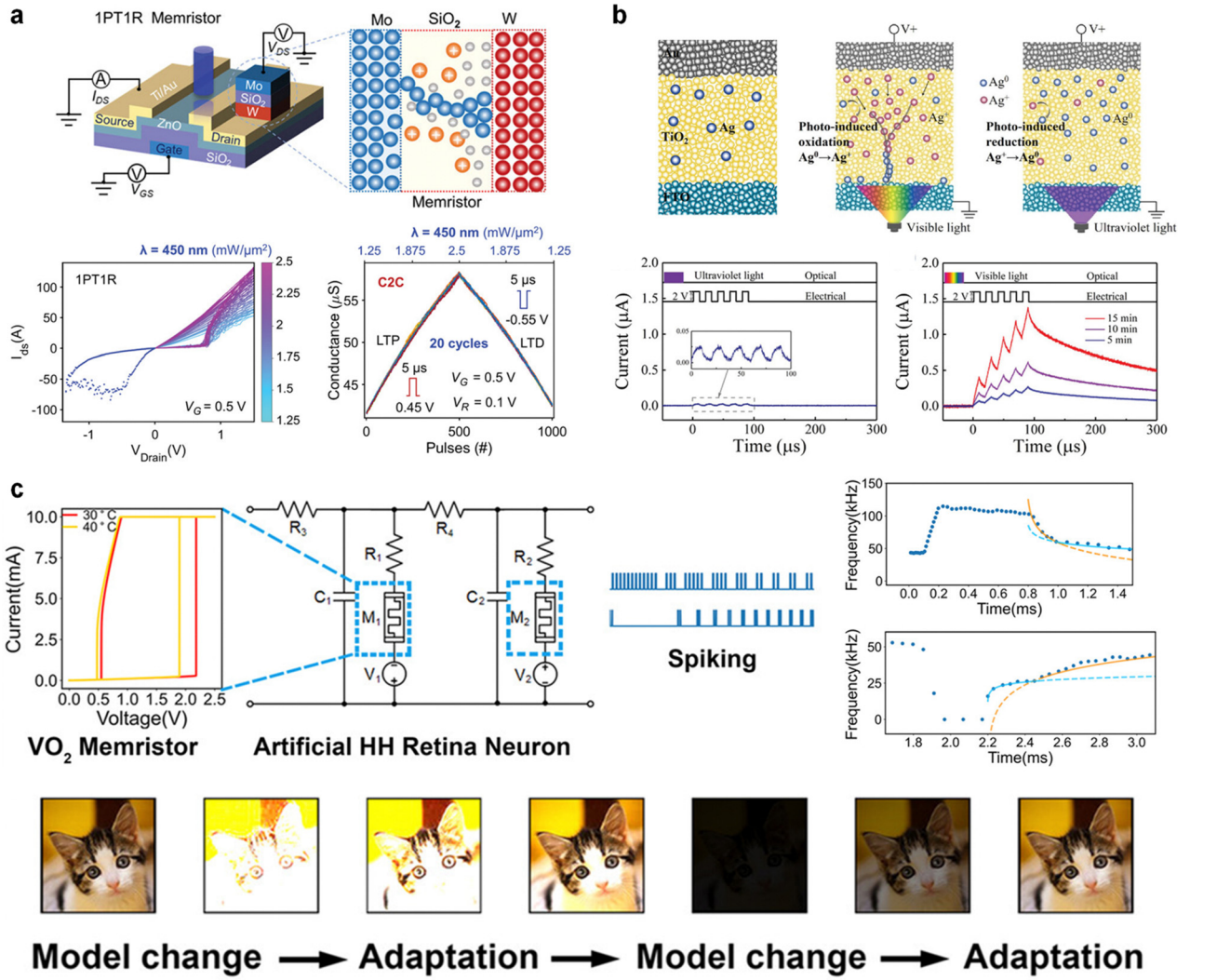

Fig. 5 (a) Schematic illustration of the integrated 1PT1R structure device and light-tunable conductance update performance of the device. Reproduced with permission from ref. 93. Copyright 2023 John Wiley and Sons. (b) Schematic illustration of a light-induced synaptic modification mechanism based on photo-induced redox reaction and current response after UV/vis light irradiation. Reproduced with permission from ref. 94 Copyright 2021 John Wiley and Sons. (c) Bio-inspired HH neurons for an artificial retinal system with firing frequency modulated in a manner similar to photopic/scotopic adaptation of a biological photoreceptor. Reproduced with permission from ref. 95. Copyright 2022 John Wiley and Sons.

conducted using UV/vis light. The memristor effectively eliminates image noise owing to its specific UV light-induced long-term depression (LTD) function. In addition, light-induced STDP learning has been identified as a feature of high-level image processing. By incorporating low-level image preprocessing steps, such as contrast enhancement and noise reduction, the learning rate and efficiency of high-level image recognition processes can be significantly improved by these memristors, as demonstrated through simulations.

Xu *et al.*[95] reported the HH neuron-based artificial visual sensory system shown in Fig. 5c constructed using a volatile VO_2 memristor. The volatile VO_2 memristor modulates the threshold and hold voltages based on temperature, which mimics a biological neuron. The proposed volatile memristor exhibits frequency relaxation in tonic spiking (a type of neuron spiking model) under varying pulse inputs, and a transition between spiking models when the input pulse changes abruptly. This is analogous to the light-adaptive functions of photoreceptors (cone and rod cells) in the retina. Primary photoreceptors responsible for light processing change during the transition between bright and dark environments. This shift, referred to as photopic and scotopic adaptation, has been successfully realized in a circuit comprising an HH neuron, a thermoelectric ceramic, and a light-dependent resistor. These components convert light into thermal stimuli that are subsequently used to generate input pulses that induce frequency changes during spiking. This light-adaptable function is useful for artificial applications. The authors demonstrated the potential of integrating spiking neural network (SNN) algorithms into machine vision applications to simplify circuits and complex processing.

4.2. Self-protection *via* detecting the intensity of light

In addition to light detection, the visual system should also be capable of analyzing the diverse spatiotemporal patterns of

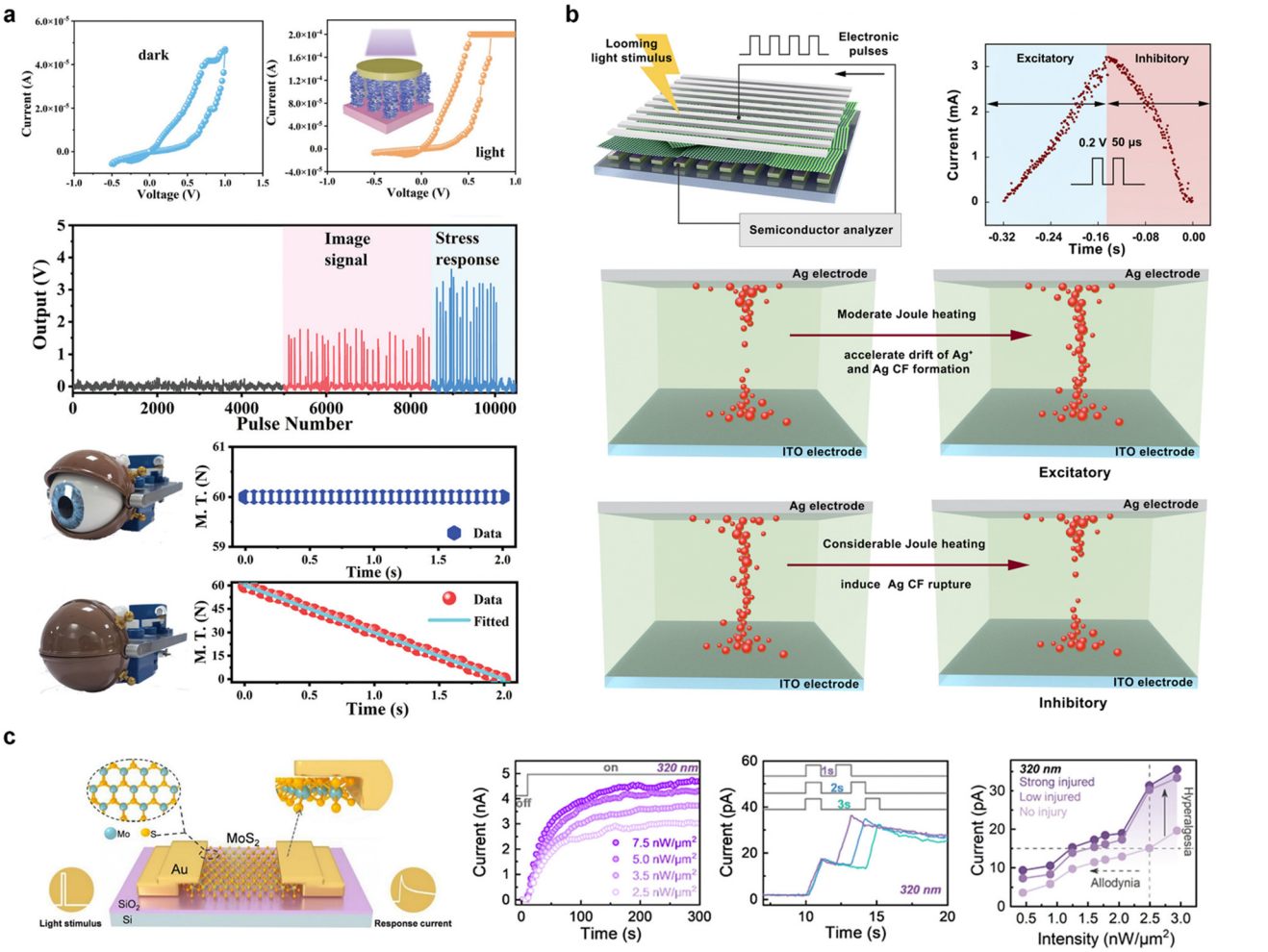

Fig. 6 (a) Multifunctional artificial visual perception nervous system constructed using an optoelectronic memristor based on an Sb_2Se_3 nanorod array. Increasing ON/OFF resistance ratio under light irradiation increases the firing frequency, activating an eyelid-shaped actuator. Reproduced with permission from ref. 96. Copyright 2022 John Wiley and Sons. (b) Schematics of the artificial LGMD neuron device and current response under looming light stimulus. The formation of the Ag conductive filament is initially facilitated by the increasing light stimulus but ruptures due to Joule heating beyond a certain light intensity, providing information before the collision point. Reproduced with permission from ref. 97. Copyright 2021 Springer Nature. (c) Schematic of the monolayer MoS_2 device and current response under varying light intensity, pulse interval, and degree of injury. Reproduced with permission from ref. 98. Copyright 2024 American Chemical Society.

photoreceptors activated in the retina. This involves protective behaviors such as closing the eyes to shield against damage from intense light and impending collisions, and nociceptive functions to detect harmful light stimuli.

A highly efficient artificial visual sensory system comprising an optoelectronic threshold-switching memristor and an actuator was proposed by Pei *et al.*[96] The Sb_2Se_3/CdS-core/shell nanorod array-based (SC) optoelectronic memristor enhanced light-harvesting activities, received optical signals, and converted them to a voltage before transmitting them to the threshold-switching memristor-based neuron circuit. The SC memristor exhibited resistive switching characteristics in a light-irradiated environment, as shown in Fig. 6a, driven by conductive dangling bonds and vacancy defects on the surface of the Sb_2Se_3 nanorods. This results in an increased ON/OFF resistance ratio, which in turn increases the firing frequency of neuronal circuits proportional to the light intensity. When the light exceeded the safety range, the firing frequency and amplitude of the SC memristor and neuron circuit increased significantly, potentially triggering an electric actuator. This emulates eye muscle contraction and reproduces the self-protective behavior of closing eyes in response to intense light damage.

Wang *et al.*[97] developed an artificial visual sensory system motivated by locusts, which, compared to humans, have a superior perception of moving objects. The vision system of locusts includes a lobular giant movement detector (LGMD) that generates danger signals before the occurrence of collisions. This functionality is demonstrated in Fig. 6b using an Ag conductive filament-based threshold-switching memristor. The formation and rupture of Ag conductive filaments in the volatile memristor were used to implement the excitatory and inhibitory effects on LGMD neurons. The conductivity of the volatile memristor increased and then decreased as the intensity of light increased. When the light power applied to the device was gradually

increased to correspond to the approaching objects, the current response initially increased, reached a peak, and then decreased as the collision point approached. In detail, at low light intensities, moderate Joule heating accelerates the drift of Ag^+ ions and the formation of conductive filaments, while at high light intensities, significant Joule heating induces the rupture of Ag conductive filaments. Consequently, the LGMD neuron implemented in this configuration provides information prior to the collision point, enabling self-protective behavior.

Li *et al.*[98] demonstrated a visual nociceptor based on a two-terminal optical synaptic device with a monolayer MoS_2 depicted in Fig. 6c. The optical synaptic device successfully emulated adjustable synaptic behaviors, including STP, LTP, and paired-pulse facilitation (PPF), by leveraging the persistent photoconductivity resulting from charge trapping. Notably, when the device was stimulated with light intensities ranging from 2.5 to 7.5 nW μm^{-2}, the photocurrent reached a higher level of saturation, which aligned with the no-adaptation characteristic of nociceptors. Furthermore, when paired 320 nm light pulses were applied to the optical synaptic device at intervals of 1, 2, and 3 s, a stronger photocurrent was observed at shorter intervals, demonstrating the dependence of the device on the relaxation time. Additionally, ultraviolet pulses with a wavelength of 320 nm and power densities of 25 and 75 nW μm^{-2} were used to induce low-injured and strong-injured states, respectively. In these injured states, the device exhibited a heightened sensitivity to light pulses. In the low-injured state, even a low-intensity ultraviolet pulse (1.5 nW μm^{-2}, 1 s) exceeded the activation threshold, while in the strong-injured state, an intensity of 1.2 nW μm^{-2}, which is below the threshold, produced a significant photocurrent. This behavior mirrors the nociceptor characteristics of ''allodynia'' and ''hyperalgesia,'' where subthreshold stimuli can elicit a response in an injured state.

To implement artificial visual sensory systems, memristors have been integrated with separate photodetection devices or fabricated using photoresponsive materials. While integration with separate devices ensures reliable processing of external stimuli, photoresponsive memristors offer superior integration density. However, incorporating photodetection capabilities into memristors often requires additional fabrication steps, such as coating nanorod arrays with photoactive materials or using ultrathin channel materials like nanosheets, which increases complexity. Therefore, further research is required to develop simplified fabrication techniques for photoresponsive memristors.

5. Memristor-based auditorial sensory systems

The biological auditory system detects and collects information from pressure waves of different amplitudes, frequencies, and components in the medium generated by motion or collision.[99–101] Sound waves that arrive at the ear are mechanically transmitted to sensory hair cells in the cochlea, generating amplified electrical signals owing to mechanical vibrations. Information in the form of amplified electrical signals is transmitted from the auditory sensory nerves to the cerebral cortex. Through this process, humans recognize sounds in their surroundings. The input sound is encoded as a train of electrical pulses created from the output of a frequency-selective channel in the cochlea (space-to-rate encoding). Sparse sampling of the frequency information was performed according to the active frequency channel without capturing all information from the sound source at the maximum sampling rate. Using this coding strategy, the cerebral cortex efficiently extracts key information from complex sound signals, enabling the biological auditory system to produce higher-level perceptions including sound location, rhythm perception, pitch recognition, and sound recognition. The ear receives a combination of simultaneous sound sources with various frequency components. This complexity is further exacerbated because both the frequency and amplitude of these components can be converted into a single sound. Owing to the spatiotemporally encoded nature and time dependency of sound waves, signal processing in the auditory system is more complicated than that in the visual or tactile systems. This section introduces the pioneering demonstration of an integrated memristor-based artificial auditory system and is divided into two subsections: sound location (azimuth detection) and sound recognition.

5.1. Sound location

To determine the location and direction of a sound source, the human brain relies on interaural time difference (ITD), which is the difference in the time of sound arrival between the two ears. The sound signal is generally divided into a left and right signal to be processed, and the important clue for sound location is the ITD in the range of −0.6 ms to 0.6 ms. Based on ITD theory, several successful demonstrations of sound localization have been conducted using memristors.

To emulate sound localization based on the ITD, Sun *et al.*[102] demonstrated precise temporal computation for the identification of acoustic sound locations using the intrinsic synaptic capability of short-term synapses. Based on the Joule heating and versatile doping-induced metal–insulator transitions in a scalable monolayer MoS_2 device, synaptic computation was conducted to process a given acoustic signal, as shown in Fig. 7a. The memristor device was designed with a biologically comparable energy consumption (10 fJ), and tunable STP was demonstrated by the flexible doping level of MoS_2. A circuit with this tunable synaptic device achieved ITD detection, emulating precise temporal computations in the human brain by suppressing the sound intensity- or frequency-dependent synaptic connectivity.

The integration of piezoelectric micromachined ultrasound transducer (pMUT) sensors into a neuromorphic RRAM-based computational map has been reported to demonstrate real-world sensory processing in object localization.[103] As shown in Fig. 7b, an event-driven auditory processing system applied to object localization was developed using an in-memory computing architecture. Inspired by the neuroanatomy of the barn owl, which is known to be an efficient auditory localization system with hunting capabilities during the night, the time-of-flight (ToF) of the sound wave was encoded, and the difference between the two ToF measurements (ITD) was analyzed to identify the sound location. The energy

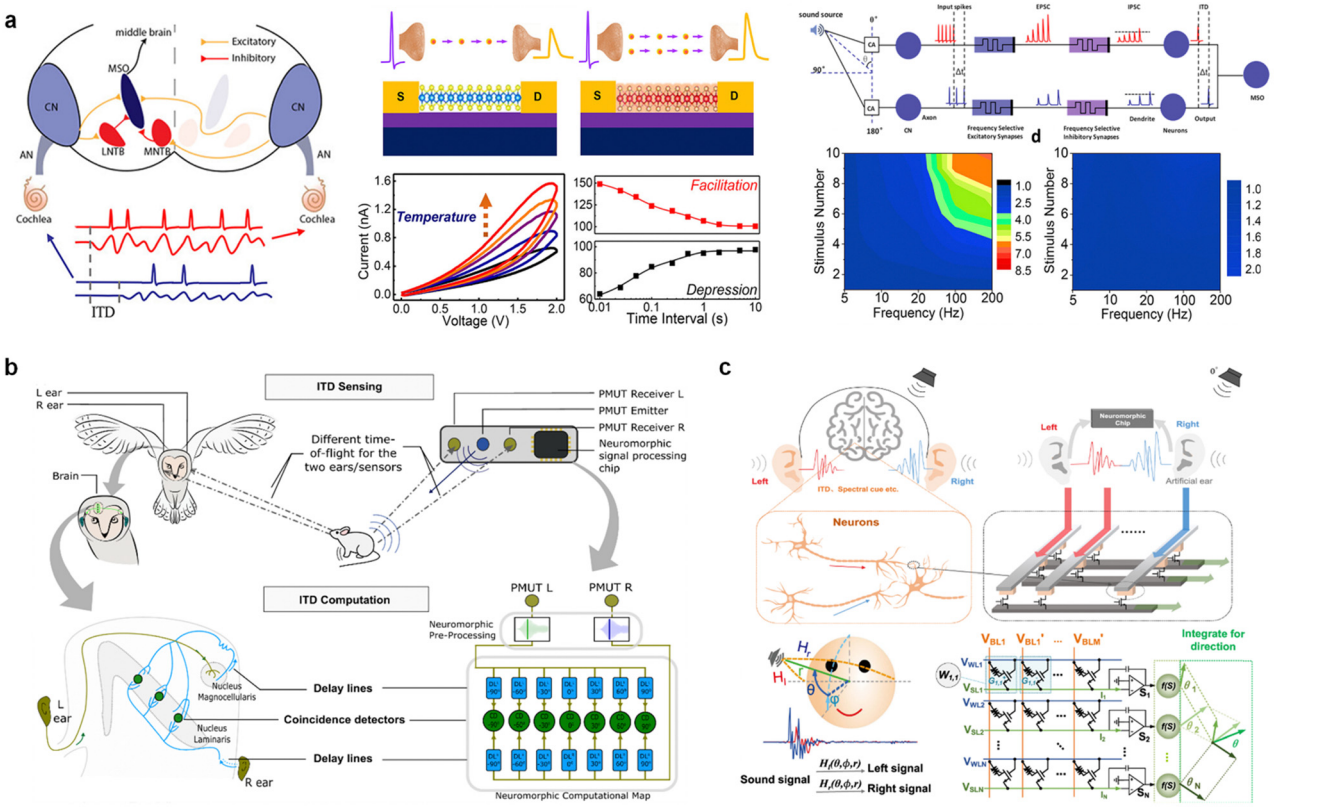

Fig. 7 (a) Schematic of the human auditory perception system and monolayer MoS_2-based device with Joule heating-driven conductance facilitation. ITD-based sound localization can be achieved by suppressing interference and encoding only ITD information through artificial synaptic computation comprising the MoS_2 device. Reproduced with permission from ref. 102. Copyright 2021 American Chemical Society. (b) Object localization system in barn owls and proposed bio-inspired technology. Response varies across population, impacting both input gain and time constant. Owing to neuron-to-neuron variability, two output neurons of a direction-sensitive coincidence detector respond differently to input stimuli. Thus, the sound source can be identified. Reproduced with permission from ref. 103. Copyright 2022 Springer Nature. (c) Conceptual diagram of a memristor-based neuromorphic sound localization system. Multiple binaural features applied for neural processing to detect sound sources, including binaural time difference, spectral shape, *etc.* Reproduced with permission from ref. 104. Copyright 2022 Springer Nature.

efficiency of object localization was realized by exploiting event-driven RRAM-based neuromorphic circuits that processed the signal information produced by the embedded sensors to calculate the position of the target object in real time. Unlike conventional sensory systems that continuously sample and calculate the detected signal to extract useful information, this energy-efficient auditory system performs asynchronous computations as useful information arrives.

Moreover, with the integrated 1 K HfO_x-based analog memristor array and a multithreshold update scheme, the *in situ* learning ability of the sound location function was demonstrated.[104] As shown in Fig. 7c, a brain-like learning algorithm and architecture for the sound location function were successfully realized, demonstrating the capability of processing sound signals from two artificial ears. With high accuracy (45.7%) and energy efficiency (184×) compared to existing methods, it demonstrated a significant advancement toward realizing advanced auditory localization systems.

5.2. Speech recognition

Speech recognition, a key requirement for artificial intelligence machines to communicate with humans, has been widely developed in software-based neural networks. However, the long latency and large storage requirements for large amounts of voice data in speech recognition tasks in the existing von Neumann architecture pose limitations. Therefore, energy-efficient neuromorphic computing systems have a significant potential for processing audio signals. In this subsection, several memristive-based artificial auditory systems with highly accurate and efficient speech recognition performances are presented.

A TiN/HfO_x/TaO_x/TiN memristor device that features a multilevel analog resistive state was developed.[105] The artificial cochlea-based circuit was used to experimentally demonstrate the filtering behaviors of five channels with different central frequencies. Consequently, when connected to a convolutional neural network, as shown in Fig. 8a, it achieved the extraction of speech features, demonstrating the feasibility of a highly efficient artificial cochlear system.

An artificial van der Waals hybrid synapse was developed and demonstrated using acoustic pattern recognition. Its superior conductance controllability was achieved using WSe_2 and MoS_2 hybrid channels, which are specialized for linear and symmetric conductance change characteristics.[106] The hybrid

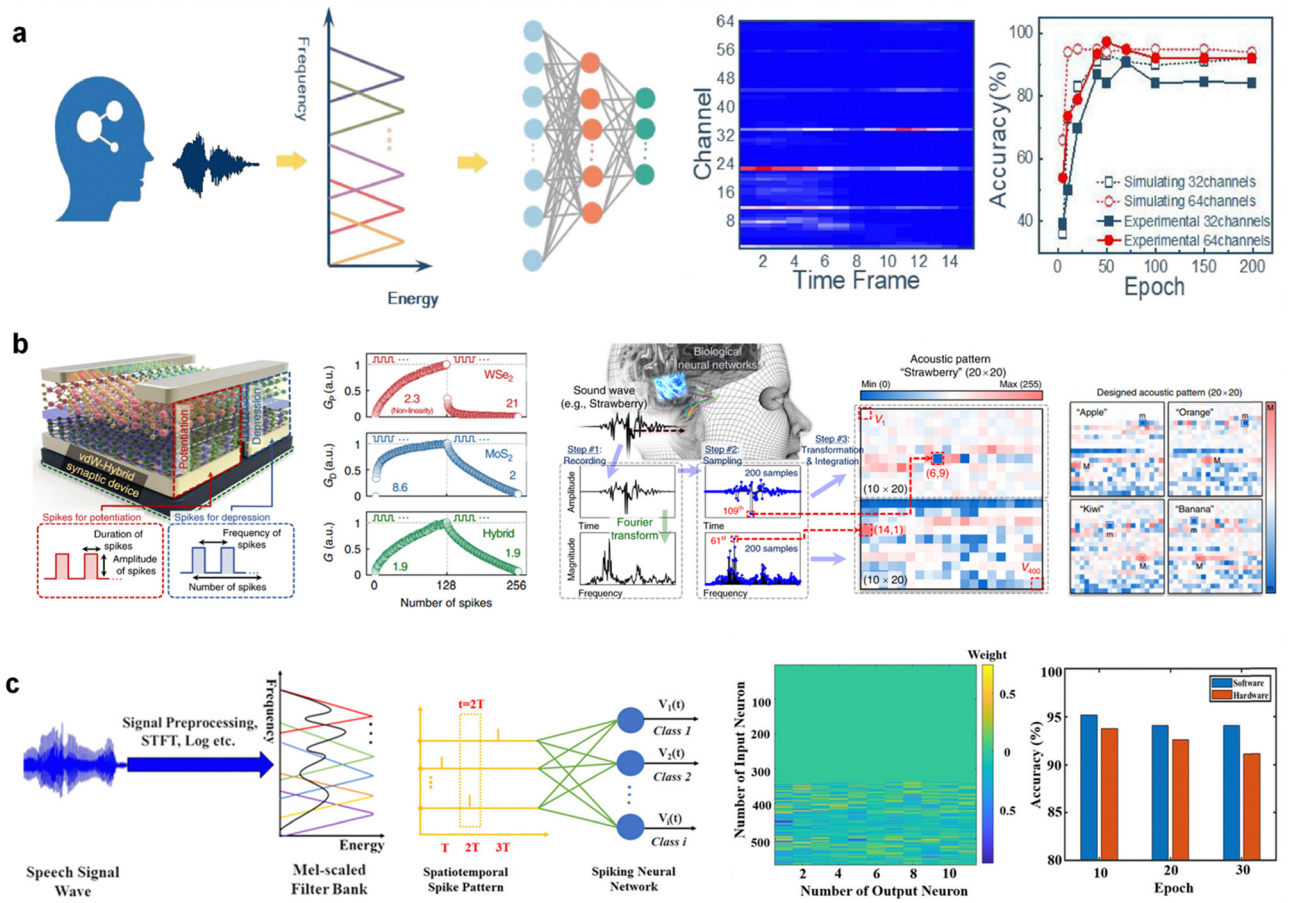

Fig. 8 (a) Schematic of an artificial cochlea speech recognition system used to demonstrate frequency-selection function of five channels in the cochlea. Channels have central frequencies determined by the resistance of a memristor. It achieved a recognition accuracy of 92% using 64 channels. Reproduced with permission from ref. 105. Copyright 2022 Frontiers Media S.A. (b) Design procedure of acoustic patterns (from recording, through transforming, to integrating). The van der Waals hybrid synapse was utilized to perform acoustic pattern recognition, a common task in speech and sound processing. Reproduced with permission from ref. 106. Copyright 2020 Springer Nature. (c) Schematic of feature extraction from speech signals. Extracting features from speech signals enables successful training of SNNs in both software- and memristor-based implementations, resulting in accurate classification inference. Reproduced with permission from ref. 107. Copyright 2021 John Wiley and Sons.

synaptic device was used to perform acoustic pattern recognition (from recording, transforming, and integrating) with high accuracy (93.8%), as shown in Fig. 8b, indicating its potential for brain-inspired computing.

Speech recognition using a memristor array (W/MgO/SiO_2/Mo) with multilevel conductance has also been demonstrated (Fig. 8c).[107] Speech recognition in a memristive SNN was achieved by precisely tuning the weights of the artificial synapses. For effective and sparse spatiotemporal feature extraction, a one-dimensional self-organizing map (SOM) network was used, which essentially operated to achieve high performance and simplify the SNN classifier. Compared to other ANN-based systems, the advantages of a simplified structure and high energy efficiency have been demonstrated in memristive SNNs for speech recognition tasks.

Memristors have demonstrated excellent performance in converting acoustic signals into electrical signals for artificial auditory sensory systems. However, a significant portion of the processing, such as post-processing and learning of the converted signals, still relies heavily on software-based computations and simulations. Additionally, there is potential for applications that can reduce sensitivity or block sounds in response to sudden loud noises, but further research is needed to explore and develop these possibilities.

6. Memristor-based olfactory sensory systems

The integration and coordination of the olfactory receptors, cortex, and muscles enables humans to recognize and memorize odor stimuli and respond to specialized gases. In the biological olfactory sensory system, odorants from the environment are detected by olfactory receptors, which trigger electrical signals as the output. Spike signals are generated by the olfactory sensory neurons and transmitted through the olfactory bulb, where signal preprocessing is performed. Finally, the preprocessed signals are transmitted to higher regions of the brain (olfactory cortex) to identify and memorize odors.[108–112]

Among the various perceptions, olfaction is particularly complex and vague because of the complexity of the chemosensory system, which must distinguish and quantify gas molecules in constantly changing environments. Therefore, these olfactory processes can provide information on complex smells, which in turn can provide key guidance for awareness, decision-making, and action in the surrounding environment.

Despite the importance of the olfactory system, relatively few studies have been conducted because of its complexity. It remains a challenge to completely emulate the functions of the human olfactory system in recognizing, memorizing, and inducing muscle movements in response to dangerous gases. Section 6 introduces various artificial olfactory systems based on the functions of the human olfactory system, including odor recognition, memorization, and protection in dangerous and gaseous environments.

6.1. Odor recognition and memorization

The olfactory system, comprising thousands of different types of receptors and classifiers, enables humans to recognize and memorize odors. Stimulated by odorant molecules, specific spikes are generated by the olfactory receptors and analyzed using neural networks. Following learning and training, humans recognize different odors through memorization using olfactory systems. Although various strategies have been proposed to construct artificial olfactory systems, most studies have focused on developing systems that use gas sensors and complex neural networks. Recently, a bioinspired memristor-based olfactory system with perceptual learning and memorization abilities was developed to classify several different gases.

Qifeng Lu *et al.* developed a hybrid flexible gas-detection system utilizing NiO nanowall-based gas sensors, oscillators, and graphene-based memristor-based synapses. In this system, the signals generated by the gas sensor are converted into pulses by an oscillator, and the frequency of these pulses varies based on the resistance of the gas sensor. The stimulation of H_2S gas at various concentrations was converted into pulse signals.[113] The altered pulses became presynaptic signals transmitted to the synaptic devices, resulting in changes in the resistance (synaptic weight) of the graphene-oxide-based synapse memristor. Resistance modulation influences information processing and storage using synaptic memristors. The system implements learning capabilities based on the *k*-nearest neighbor (KNN) algorithm, which efficiently categorizes unknown gas stimuli into the most probable categories by comparing them with pre-learned boundaries. The gas-detection system demonstrated enhanced recognition capabilities through iterative learning. Initially, the error rate exceeded 45%; however, as the number of learning iterations increased, the error rate progressively decreased to approximately 20%. This methodology enhances the practical application of gas-detection systems and ensures reliable data analysis.

In addition to the mere recognition of a single gas, olfactory systems have been reported to enable the detection of various gases.[114] The reported system utilizes an array of gas sensors along with neurons and synapses to form an olfactory sensory system capable of effectively analyzing complex gaseous environments. An array of gas sensors capable of detecting four different gases (formaldehyde, ethanol, acetone, and toluene) at various concentrations were used to effectively monitor diverse gaseous environments. In a gaseous environment, the resistance changes in each sensor adjusted the intensity of the voltage applied to the series-connected neuronal memristor (Pt/Ag/TaO_x/Pt) (Fig. 9a). These modifications to the input voltage translate the chemical information of the gases into electrical spikes in the neuron memristors, thereby providing information on the gas-detection capabilities of the entire system. The spikes generated in each neuron are transmitted to a synaptic array (Pt/Ta/TaO_x/Pt), where they undergo learning and training through spike rate-dependent plasticity (SRDP). This process enables the storage of gas characteristics in memristor devices. Based on matrix-vector multiplication, the system can effectively classify four different types of gases. This system enables the precise identification and quantification of gases with distinct chemical properties, which is highly beneficial for environmental monitoring. Furthermore, these memristor-based sensory systems overcome efficiency problems encountered in existing artificial sensory systems, such as frequent sampling, data storage, and transfer. Han *et al.* reported that sensors with differing sensitivities to the same gas were serially connected to memristor-based neurons, proposing an olfactory system capable of clearly recognizing and differentiating mixed gases.[115] In this system, gas exposure alters the resistance of the gas sensors, modifying neuronal frequency, which can be used for gas detection. Sensors based on SnO_2 and WO_3 exhibit different resistance changes in response to the same gas, leading to distinct neuronal firing frequencies. This configuration enables the artificial olfactory system to distinguish unknown gases more accurately. Furthermore, integration with SNNs has enhanced the ability of the system to identify various types of reducing gases (NH_3, CO, acetone, and NO_2). The introduction of additional hidden layers in the SNNs further improves the recognition of more complex gas mixtures, highlighting their potential for environmental monitoring and safety applications.

Currently, gas recognition and memory require additional gas sensors and circuits, which adversely affect the power consumption and miniaturization of the device. Chun *et al.* reported a system capable of recognizing and remembering gases without requiring additional devices or circuits by employing materials in synaptic memristors that exhibited both gas-detection capabilities and resistive change properties, as depicted in Fig. 9b. A synaptic memristor based on Pt/TiO_2 NR/TiN can directly detect gases and remember them through changes in the resistance state.[116] The TiO_2 material, the oxide layer of synaptic devices, is not only used for resistive switching in synaptic memristors but is also employed for gas detection in conventional gas sensors. When a synaptic memristor is exposed to H_2 gas, the gas reacts with TiO_2 to generate oxygen vacancies, promoting the growth of conductive paths and decreasing resistance. Conversely, exposure to NO gas removes oxygen vacancies, causing disruptions in conductive paths and

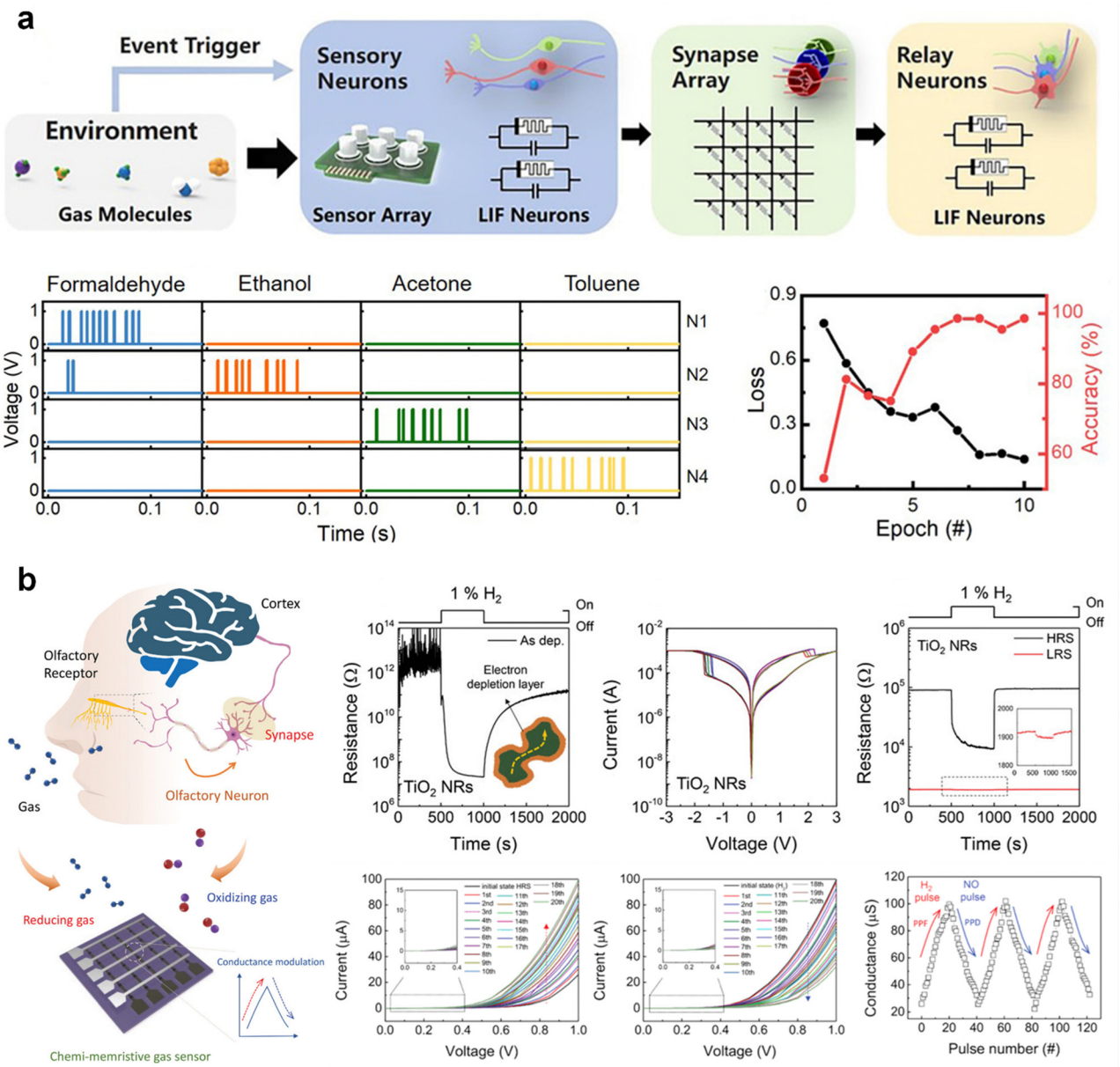

Fig. 9 (a) Bio-inspired neuromorphic olfactory system based on the memristive neural network comprising a gas sensor, sensory neurons, synapse arrays, and relay neurons. Sampling voltages in the LIF neuron. Larger input signals (red lines) result in shorter capacitor charging times (green lines), quicker device switching (blue lines), and higher output frequencies (orange lines). Training loss and testing accuracy of detection gas. Reproduced with permission from ref. 114. Copyright 2022 John Wiley and Sons. (b) Schematic of biological olfactory cognitive process mimicking using a chemi-memristive sensor. Response curves upon exposure to 1% H_2 and I–V curves of TiO_2 NRs. Conductance modulations based on the type of target gas (reducing or oxidizing). Reproduced with permission from ref. 116. Copyright 2023 John Wiley and Sons.

increasing the resistance. The synaptic device detects changes in resistance due to gas exposure and stores information regarding the exposure. This process enables accurate recording of information related to gas detection and provides reliable environmental monitoring. This technology plays a crucial role in measuring and managing gas concentrations in various environments. In addition, the gas detection capability of a single memristor can be effectively applied to mixed-gas recognition. Beyond conventional gas-sensor arrays, a new approach has been reported to leverage the unique gas selectivity of various materials to construct memristor arrays. This study utilized SnO_2, HfO_2, and Ta_2O_5-based memristors, which exhibit resistance changes in response to gas interactions. These memristors demonstrated varying sensitivities to specific gases and concentrations, enabling the simultaneous detection of mixed gases. A parallel array significantly improved the accuracy of mixed-gas concentration predictions, outperforming single-device systems by over 796% compared to individual Ta_2O_5-based sensors. This advancement underscores the potential of memristor-based sensor technology to enhance

environmental monitoring and improve the accuracy and reliability of gas detection in complex gas environments.[117]

6.2. Protection in dangerous gas environments

The olfactory system plays a crucial role in human awareness, perception, and action in response to diverse external gaseous stimuli. The coordination of olfactory receptors and muscles enables humans to respond to specific gases, which is crucial for protection in dangerous environments, such as in the case of leakage of toxic gases or rooms on fire. However, studies on the functions of the human olfactory system based on memristor devices involving perception, memorization, and self-protection movements are lacking. To emulate a complete olfactory system, an artificial olfactory system should be developed to memorize gas information and control muscles to ensure self-protection in dangerous environments.

Recently, bioinspired olfactory systems that enable the perception and memory of specific gases with the ability to act in the presence of certain gases have been reported. Gas-sensing visualization using a smart robot was developed for real-time gas monitoring by integrating gas sensors and memory devices (Fig. 10a).[118] The robot was equipped with an artificial olfactory memory system developed to recognize and memorize volatile organic compound (VOC) gases at different concentrations. The integration of the sensor and memory unit facilitated the switching of the synaptic memristor in response to the VOC gas and the recording of target gas information after the gas stimuli disappeared. Additionally, the system was reconfigured with an LED to enhance the gas detection visualization. When concentrations of VOCs were detected below the threshold, the LED remained off. However, if the VOC concentration exceeds the threshold, the LED immediately brightens and remains on. These capabilities of the olfactory system present great potential for future humanoid robots, environmental pollution control, and early warning of chemical and biohazard safety to alert and respond to emergencies in dangerous environments.

In addition to warning about hazardous gases, the flexible artificial olfactory system shown in Fig. 10b can recognize,

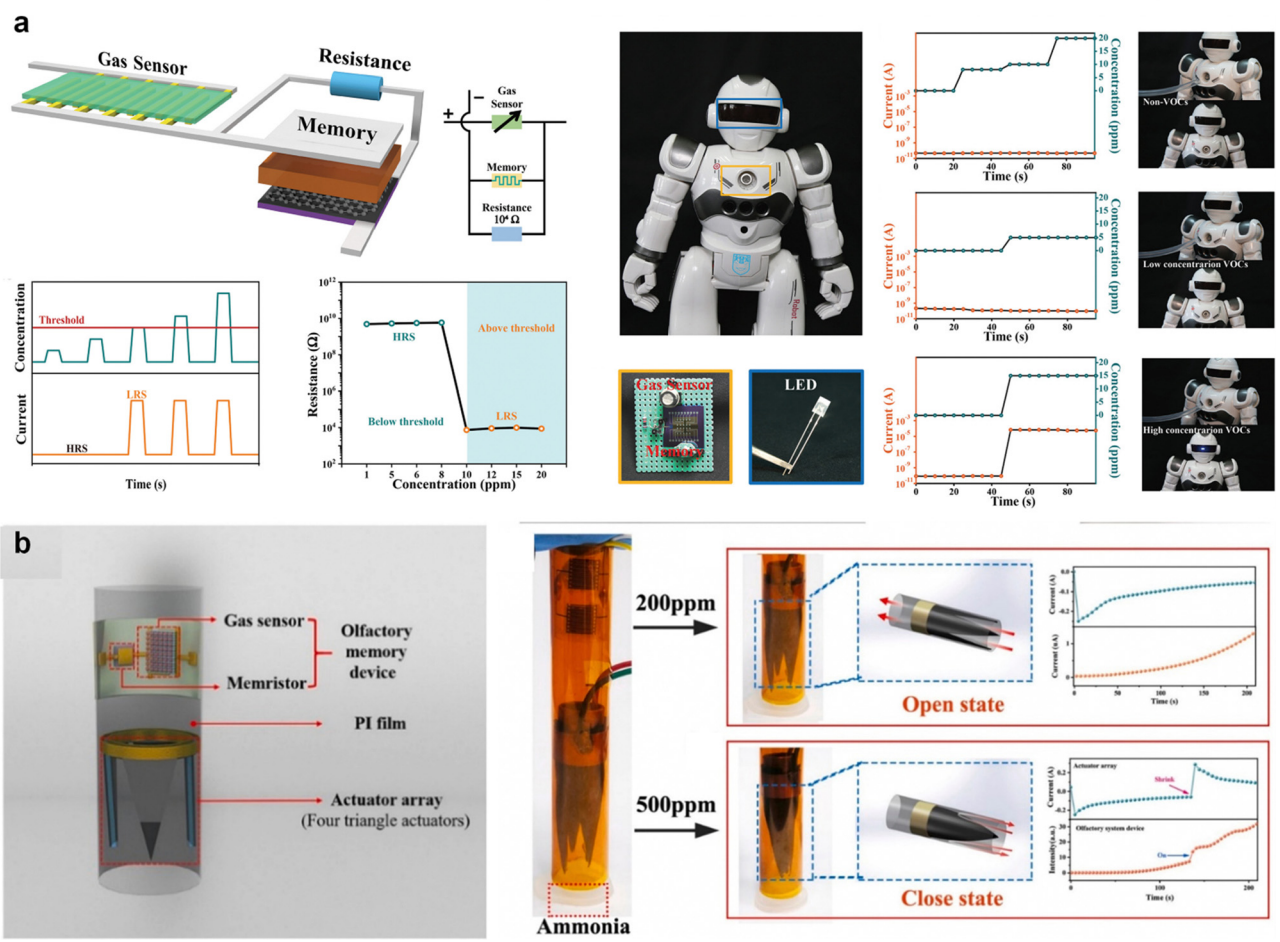

Fig. 10 (a) Sensory information provided by volatile organic compounds sensed by olfactory sensory receptors. Demonstration of a robot equipped with an artificial olfactory memory system to visualize gas sensing. Higher concentration of VOCs above threshold resulted in switching of a memory device and lighting up of an LED. Reproduced with permission from ref. 118. Copyright 2021 John Wiley and Sons. (b) Schematic illustration of nose comprised of four arc actuators. Response of the bionic nose to high concentration (500 ppm) ammonia and instantaneous current changes of an artificial olfactory system and actuator array. Reproduced with permission from ref. 119. Copyright 2021 Elsevier.

memorize, and perform self-protection actions for NH_3 and was developed by integrating Sr–ZnO-based gas sensors, HfO_x-based memristors, and electrochemical actuators.[119] The gas sensor and synaptic memristor are connected in series, such that changes in NH_3 concentration alter the resistance of the gas sensor, which modifies the voltage intensity applied to the synaptic memristor according to the voltage division rule. Thus, the external chemical signals are conveyed as changes in the electrical signals to the memristor through the resistance variation of the gas sensor. This process plays a crucial role in translating chemical stimuli into electrical signals. When exposed to specific concentrations of NH_3, the resistance of the gas sensor decreased sharply; consequently, a voltage (set voltage) sufficient to switch the synaptic memristor was applied. When the NH_3 concentration was low, the memristor remained inactive, causing the actuator to remain unresponsive and the gas to flow normally. Conversely, as the NH_3 concentration increased, the olfactory memory device was activated, causing the actuator to bend inward and close into a conical shape, thereby preventing gas from entering the nasal cavity. Thus, the activation of the memristor triggers the movement of the electrochemical actuator to block the gas flow channel, mimicking the self-protective action of the induced muscle movement of the hand when it smells NH_3.

This section highlights the effective utilization of memristor-based olfactory systems in humanoid robotics and environmental monitoring. However, these systems face inherent limitations in selectivity and sensitivity to various gases. Moreover, there is a need to develop systems that can detect external gases in real time, process the data, and execute appropriate responses. This approach facilitates rapid and accurate reactions to gas leaks and chemical hazards, significantly improving the efficiency of environmental monitoring systems.

7. Conclusions and perspectives

Memristive artificial sensory systems, inspired by the energy-efficient architecture of biological systems, have been developed to overcome the technological limitations of conventional CMOS-based systems. Memristors can emulate the receptors, neurons, and synapses—the fundamental components of biological sensory systems. Building on this foundation, memristors enable higher-order functions such as learning, inference, and hazard detection by mimicking specific biological sensory systems. Table 1 summarizes how various memristors emulate biological components and implement sensory characteristics, demonstrating that memristive artificial sensory systems can effectively replicate the four major human senses.

In this review, we suggested the emulation of receptor, neuron, and synapse properties using memristors based on an understanding of their inherent characteristics. Volatile memristors exhibit switching behavior, transitioning to an ON state when stimuli exceed a specific threshold and returning to the Off state when stimuli are removed. This behavior is suitable for simulating receptors and neurons as it closely resembles the ''threshold'' and ''relaxation'' responses of biological receptors. In addition, by adjusting stimulus intensity and duration, volatile memristors can replicate biological phenomena such as adaptation and sensitization. Moreover, their behavior closely resembles ''the ion channel dynamics'' observed in neurons. When connected to an external circuit, volatile memristors can effectively model spike generation, including LIF and HH models, as well as neuron spike shapes. Non-volatile memristors, by contrast, alter their resistance in response to an applied bias and retain their resistance even after the bias is removed. This characteristic allows them to mimic the information storage function of biological synapses, where resistance modulation corresponds to ''synaptic weight'' adjustments in response to neural stimuli.

Table 1 A summary of memristive artificial sensory systems

Sense	Memristor	Materials & structure	Biological counterpart	Specific feature	Ref.
Tactile	Non-volatile	Ag/$CsPbBr_3$/PVA/FTO	Synapse	Mechanoreceptor (pressure)	120
	Non-volatile	Al/CS:MWCNTs/ITO	Synapse	Mechanoreceptor (pressure)	121
	Non-volatile	Ag/TiO_x/$Ti_3C_2T_x$/Au	Neuron	Mechanoreceptor (pressure)	122
	Volatile	Al/ZnO/FTO	Synapse	Nociceptor	123
	Volatile	Ag/c-YY NW/Ag	Neuron	Mechanoreceptor (humidity)	124
Visual	Volatile	Al/Ag NW-embedded SA/SA/ITO	Synapse/neuron	Scotopic/photopic adaptation	125
	Volatile	Cr/Au/WS_2/Cr/Au	Synapse	Color recognition	126
	Volatile	ITO/Ta_2O_5/Ag/IGZO/ITO	Neuron	Color recognition	127
	Volatile/non-volatile	FTO/NiO/Organic Interlayer/PMMA/Ag	Synapse	Color recognition	128
	Volatile/non-volatile	Pd/TiO_x/ZnO/TiN	Synapse	Object tracking	129
Auditory	Volatile	Pd/Nb/NbO_x/Nb/Pd	Synapse	Sound localization	130
	Non-volatile	TiN/TaO_y/HfO_x/TiN	Synapse	Sound localization	131
	Non-volatile	TiN/HfO_x/Ti/TiN	Synapse	Object localization	132
	Non-volatile	Pt/TiO_x/AlO_x/Pt	Synapse	Audio-reward association	133
Olfactory	Non-volatile	Ta/m-ZrO_2/Pt	Synapse	Odor recognition	134
	Non-volatile	Al/pectin:Ag NPs/ITO	Synapse	Odor recognition	135
	Volatile/non-volatile	W/WO_3/PEDOT:PSS/Pt, Pd/W/WO_3/Pd	Synapse/neuron	Gas-classification	136
	Non-volatile	—/TiO_2 Nanowire/Ti	Sensor	Odor recognition	137

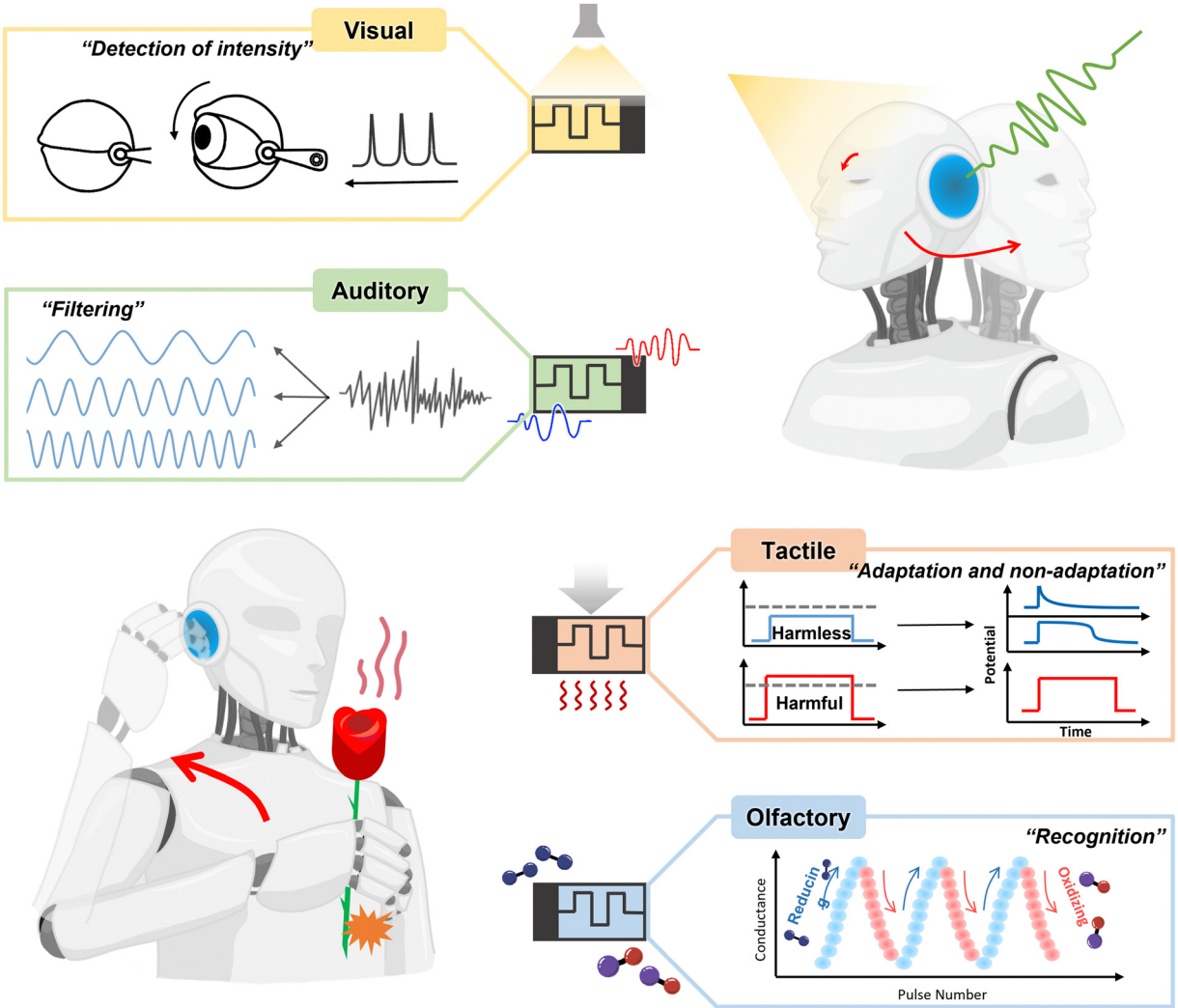

Fig. 11 Schematic of biological and artificial sensory systems with a memristor.

We then discuss the implementation of the four major senses—tactile, visual, auditory, and olfactory—in the memristor-based artificial sensory system, as illustrated in Fig. 11. Notably, memristors enable comprehensive coverage of previously unachievable functionalities that play crucial roles in sensory systems and offer efficient energy consumption compared to CMOS-based devices and memristors (Table 2). In artificial tactile systems, advancements in memristor material and structural design have enabled the effective emulation of receptor characteristics such as "sensitivity" and "adaptability," which were previously challenging to emulate. For example, the system demonstrates a function in which the output gradually decreases in response to innocuous stimuli. This contradicts the conventional belief that reliable signal conversion requires a consistent output for identical inputs. This aligns with the operational tendencies of biological sensory systems. In the artificial visual system, memristors emulate neuron-spiking models with high precision to simulate the functions of biological photoreceptors. By reducing the output in response to sudden increases in input signals, the system facilitates "light intensity detection" and "self-protection." Notably, it efficiently extracts and delivers only essential information for actions, such as collision avoidance or blinking, from vast visual data inputs. Furthermore, while nociceptors have predominantly been implemented for tactile stimuli, the development of nociceptive functionality that is responsive to visual stimuli is particularly remarkable. In the artificial auditory system, the memristors are connected to additional circuits that emulate the filtering function of the cochlea. This system is designed to recognize only specific sound amplitudes based on memristor resistance, enabling "speech recognition" in the biological auditory system. This represents a significant advancement in artificial auditory systems. In the artificial olfactory system, memristors fabricated from gas-sensitive materials integrate sensing and switching characteristics. This approach allows the detection of external stimuli without an additional circuit. Furthermore, memristor resistance varies depending on gas type, allowing for

Table 2 Comparison of switching characteristics with CMOS-based devices

		Structure	Operating voltage	Switching speed	ION	Ref.
Receptor	CMOS	Sn-doped polycrystalline β-Ga_2O_3 FET	10 V (VD)	0.5 s	—	138
	Memristor	Ag/SnSe/Au	Set: 0.474	55 ns	10 μA	139
		Pt/Ag/SiO_2 NRs/Ag/Pt	Set: −0.72 V +0.78 V	20 μs	1 μA	78
Neuron	CMOS	Si-based MOSFET	V_G: −1 V V_D: >3.5 V	0.1 s	≈150 μA	140
		Si/SiO_2/Si_3N_4/SiO_2/Si-based MOSFET	V_G: 12 V V_D: >3 V	0.02 s	≈150 μA	141
	Memristor	Pt/Ag/TaO_x/Pt	Set: 0.29 V	80 μs	0.1 μA	114
		Ag/MoS_2 nanosheet/Ag/MoO_x/Ag	Set: 0.3 V	16 ns	100 μA	31
		Pt/Ag/ZnO/Pt	Set: 0.17 V	≈50 ns	10 μA	142
Synapse	CMOS	Si/WO_x/SiO_2-based FET	Write: 1.8 V (V_G) Erase: −2.5 (V_G)	0.3 ms	—	143
		IGZO channel-based FET	Write: 20 V (V_G) Erase: −20 V (V_G)	100 ms (write) 10 ms (erase)	≈10 μA	144
	Memristor	Pd/WS_2/Pt	Set: 0.6 V Reset: −0.2 V	14 ns	1 μA	145
		Al/PVP-CdSe QD/Al	Set: 0.61 V Reset: −0.5 V	41 ns	5.2 μA	146
		ITO/CdS QDs-PVP/Al	Set: 1.08 V Reset: −0.72 V	42 ns	4.44 μA	147

"recognition and memorization" of specific gases. These findings break the conventional stereotype that receptors are solely responsible for stimulus detection while synapses manage information storage. Instead, they demonstrate that bioinspired and highly efficient system architectures can perform multiple functions within a single device. Besides, conventional CMOS-based artificial neural systems struggle to implement advanced sensory functions. Even if achievable, such implementations typically require significant energy consumption and extended processing times. In contrast, memristor-based artificial sensory systems can efficiently emulate these advanced functions.

While memristor-based artificial sensory systems demonstrate extensive potential, key challenges remain to be addressed. Although progress has been made in using memristors independently to detect stimuli and mimic sensory system functions, system-level integration remains challenging. Most implementations still rely on additional sensors and circuits primarily used for signal conversion, such as translating the firing frequency of artificial neurons into a form that other components can process. However, improving the energy efficiency of this conversion process has not been well explored. Although memristors themselves consume nanojoule to picojoule-level low energy, integrating them with CMOS-based systems often introduces mismatches in electrical parameters, requiring additional circuitry for voltage conversion, signal processing, and computation. This increases system complexity and overall energy consumption, limiting memristors' ability to mimic biological sensory systems fully. Moreover, if memristors cannot be fabricated using CMOS-compatible materials and processes, chip-level integration becomes extremely challenging. Without chip-level integration, memristors and CMOS-based devices or circuits must be implemented separately, leading to undesirable consequences such as signal transmission noise, increased energy consumption, and a larger system area. For instance, Section 4.2 discussed a memristor-based model mimicking the LGMD neuron, which was integrated into a car robot to generate avoidance behavior based on optic input signals. However, implementing this system required power management chips for voltage conversion and counter circuits for spike frequency calculation, leading to a complex structure with additional energy consumption. Unfortunately, current research primarily focuses on enhancing the performance of individual memristor devices, with limited studies addressing CMOS compatibility and efficient architectures for seamless integration with CMOS-based systems. Therefore, developing a more advanced memristor-based architecture is essential to enable practical and energy-efficient system integration. Furthermore, addressing the following challenges is imperative for the advancement of artificial sensory systems. First, research on advanced data processing to perform complex tasks is required. Efficient management of spatiotemporal data requires multiple memristors working in conjunction, along with mechanisms to compare and integrate data from each device. Recent studies have primarily focused on single memristors, with limited algorithms developed for arrays or circuits. To mimic biological intelligence, it is essential to establish interconnections among memristors and integrate their functions. Additionally, research on integrated system-level memristor-based receptors, neurons, and synapses is significantly lacking. To construct artificial sensory systems, memristors emulate and integrate receptors, neurons, and synapses. However, most studies focus on them in isolation rather than as part of a cohesive system. Achieving more efficient conversion and data processing between system components is essential for accurately replicating biological sensory functions. For artificial sensory systems to function reliably, research studies must focus on compatible signal conversion between the pre- and post-components. These investigations have the potential to advance the overall integration of sensory systems by enabling electrical processing of neural signals for information transmission and ensuring accurate execution of output signals. In conclusion, this review provides a framework for implementing memristive

artificial sensory systems based on the characteristics of biological components and switching properties of memristors.

Author contributions

J. E. Kim and K. Soh conceived the review and wrote the manuscript. S. I. Hwang and D. Y. Yang reviewed the manuscript. J. H. Yoon supervised the review and finalized the manuscript. All authors have approved the final version of the manuscript.

Data availability

No primary research results, software, or codes were involved, and no new data were generated or analyzed as part of this review.

Conflicts of interest

The authors declare no conflict of interests.

Acknowledgements

This research was supported by the National R&D Program through the National Research Foundation of Korea (NRF) and the Korea Basic Science Institute (National Research Facilities and Equipment Center) and funded by the Ministry of Science and ICT (RS-2024-00406418, NRF-2022R1C1C1004176, and RS-2024-00403917).

Notes and references

1 P. K. Paritala, S. Manchikatla and P. K. D. V. Yarlagadda, *Procedia Eng.*, 2017, **174**, 982–991.
2 U. Rosolia, X. Zhang and F. Borrelli, *Annu. Rev. Control. Robotics Auton. Syst.*, 2018, **1**, 259–286.
3 Y. LeCun, Y. Bengio and G. Hinton, *Nature*, 2015, **521**, 436–444.
4 Z. Wang, S. Joshi, S. Savel'Ev, W. Song, R. Midya, Y. Li, M. Rao, P. Yan, S. Asapu, Y. Zhuo, H. Jiang, P. Lin, C. Li, J. H. Yoon, N. K. Upadhyay, J. Zhang, M. Hu, J. P. Strachan, M. Barnell, Q. Wu, H. Wu, R. S. Williams, Q. Xia and J. J. Yang, *Nat. Electron.*, 2018, **1**, 137–145.
5 P. M. Sheridan, F. Cai, C. Du, W. Ma, Z. Zhang and W. D. Lu, *Nat. Nanotechnol.*, 2017, **12**, 784–789.
6 S. Seo, S. H. Jo, S. Kim, J. Shim, S. Oh, J. H. Kim, K. Heo, J. W. Choi, C. Choi, S. Oh, D. Kuzum, H. P. Wong and J. H. Park, *Nat. Commun.*, 2018, **9**, 5106.
7 S. Chen, Z. Lou, D. Chen and G. Shen, *Adv. Mater.*, 2018, **30**, 1705400.
8 S. Kumar, R. S. Williams and Z. Wang, *Nature*, 2020, **585**, 518.
9 J. Wu, Y. Chua, M. Zhang, H. Li and K. C. Tan, *Front. Neurosci.*, 2018, **12**, 836.
10 H. Kalita, A. Krishnaprasad, N. Choudhary, S. Das, D. Dev, Y. Ding, L. Tetard, H. S. Chung, Y. Jung and T. Roy, *Sci. Rep.*, 2019, **9**, 1.
11 P. Stoliar, J. Tranchant, B. Corraze, E. Janod, M. P. Besland, F. Tesler, M. Rozenberg and L. Cario, *Adv. Funct. Mater.*, 2017, **27**, 1604740.
12 X. Zhang, J. Lu, Z. Wang, R. Wang, J. Wei, T. Shi, C. Dou, Z. Wu, J. Zhu, D. Shang, G. Xing, M. Chan, Q. Liu and M. Liu, *Sci. Bull.*, 2021, **66**, 1624.
13 I. Polykretis, G. Tang, P. Balachandar and K. P. Michmizos, *IEEE Trans. Med. Robot. Bionics*, 2022, **4**, 520–529.
14 W. Shi, J. Cao, Q. Zhang, Y. Li and L. Xu, *IEEE Internet Things J.*, 2016, **3**, 637–646.
15 A. Vanarse, A. Osseiran and A. Rassau, *Front. Neurosci.*, 2016, **10**, 115.
16 I. T. Wang, C. C. Chang, L. W. Chiu, T. Chou and T. H. Hou, *Nanotechnology*, 2016, **27**, 365204.
17 M. Prezioso, F. Merrikh-Bayat, B. D. Hoskins, G. C. Adam, K. K. Likharev and D. B. Strukov, *Nature*, 2015, **521**, 61–64.
18 S. Choi, J. Yang and G. Wang, *Adv. Mater.*, 2020, **32**, 1–26.
19 D. S. Jeong, K. M. Kim, S. Kim, B. J. Choi and C. S. Hwang, *Adv. Electron. Mater.*, 2016, **2**, 1–27.
20 H. Li, S. Wang, X. Zhang, W. Wang, R. Yang, Z. Sun, W. Feng, P. Lin, Z. Wang, L. Sun and Y. Yao, *Adv. Intell. Syst.*, 2021, **3**, 2100017.
21 J. Park, *Electronics*, 2020, **9**, 1–16.
22 R. Yang, H. M. Huang and X. Guo, *Adv. Electron. Mater.*, 2019, **5**, 1900287.
23 F. Cai, J. M. Correll, S. H. Lee, Y. Lim, V. Bothra, Z. Zhang, M. P. Flynn and W. D. Lu, *Nat. Electron.*, 2019, **2**, 290–299.
24 J. F. Yang, A. T. Liu, T. A. Berrueta, G. Zhang, A. M. Brooks, V. B. Koman, S. Yang, X. Gong, T. D. Murphey and M. S. Strano, *Adv. Intell. Syst.*, 2022, **4**, 2100205.
25 S. Wang, S. Gao, C. Tang, E. Occhipinti, C. Li, S. Wang, J. Wang, H. Zhao, G. Hu, A. Nathan, R. Dahiya and L. G. Occhipinti, *Nat. Commun.*, 2024, **15**, 4671.
26 Z. Cao, L. Xiang, B. Sun, K. Gao, J. Yu, G. Zhou, X. Duan, W. Yan, F. Lin, Z. Li, R. Wang, Y. Lv, F. Ren, Y. Yao and Q. Lu, *Mater. Today Bio*, 2024, **26**, 101096.
27 M. Rao, H. Tang, J. Wu, W. Song, M. Zhang, W. Yin, Y. Zhuo, F. Kiani, B. Chen, X. Jiang, H. Liu, H.-Y. Chen, R. Midya, F. Ye, H. Jiang, Z. Wang, M. Wu, M. Hu, H. Wang, Q. Xia, N. Ge, J. Li and J. J. Yang, *Nature*, 2023, **615**, 823–829.
28 X. Zhang, Y. Zhuo, Q. Luo, Z. Wu, R. Midya, Z. Wang, W. Song, R. Wang, N. K. Upadhyay, Y. Fang, F. Kiani, M. Rao, Y. Yang, Q. Xia, Q. Liu, M. Liu and J. J. Yang, *Nat. Commun.*, 2020, **11**, 1–9.
29 F. Li, R. Wang, C. Song, M. Zhao, H. Ren, S. Wang, K. Liang, D. Li, X. Ma, B. Zhu, H. Wang and Y. Hao, *ACS Nano*, 2021, **15**, 16422–16431.
30 Q. Wu, B. Dang, C. Lu, G. Xu, G. Yang, J. Wang, X. Chuai, N. Lu, D. Geng, H. Wang and L. Li, *Nano Lett.*, 2020, **20**, 8015–8023.
31 J. K. Han, D. M. Geum, M. W. Lee, J. M. Yu, S. K. Kim, S. Kim and Y. K. Choi, *Nano Lett.*, 2020, **20**, 8781–8788.
32 G. Indiveri, B. Linares-Barranco, R. Legenstein, G. Deligeorgis and T. Prodromakis, *Nanotechnology*, 2013, **24**, 384010.
33 G. W. Burr, R. M. Shelby, A. Sebastian, S. Kim, S. Kim, S. Sidler, K. Virwani, M. Ishii, P. Narayanan, A. Fumarola,

L. L. Sanches, I. Boybat, M. Le Gallo, K. Moon, J. Woo, H. Hwang and Y. Leblebici, *Adv. Phys.:X*, 2017, **2**, 89–124.
34 Q. Wan, M. T. Sharbati, J. R. Erickson, Y. Du and F. Xiong, *Adv. Mater. Technol.*, 2019, **4**, 1–34.
35 B. Joo, J. W. Han and B. S. Kong, *IEEE Trans. Circuits Syst. I Regul. Pap.*, 2022, **69**, 3632–3642.
36 X. Yan, J. Niu, Z. Fang, J. Xu, C. Chen, Y. Zhang, Y. Sun, L. Tong, J. Sun, S. Yin, Y. Shao, S. Sun, J. Zhao, M. Lanza, T. Ren, J. Chen and P. Zhou, *Mater. Today*, 2024, **80**, 365–373.
37 Y. Pei, L. Yan, Z. Wu, J. Lu, J. Zhao, J. Chen, Q. Liu and X. Yan, *ACS Nano*, 2021, **15**, 17319–17326.
38 Y. Pei, B. Yang, X. Zhang, H. He, Y. Sun, J. Zhao, P. Chen, Z. Wang, N. Sun, S. Liang, G. Gu, Q. Liu, S. Li and X. Yan, *Nat. Commun.*, 2025, **16**, 48.
39 S. Kumar, X. Wang, J. P. Strachan, Y. Yang and W. D. Lu, *Nat. Rev. Mater.*, 2022, **7**, 575–591.
40 F. Qin, Y. Zhang, H. W. Song and S. Lee, *Mater. Adv.*, 2023, **4**, 1850–1875.
41 Y. Zhang, Z. Wang, J. Zhu, Y. Yang, M. Rao, W. Song, Y. Zhuo, X. Zhang, M. Cui, L. Shen, R. Huang and J. Joshua Yang, *Appl. Phys. Rev.*, 2020, **7**, 1.
42 S. Kumar, R. S. Williams and Z. Wang, *Nature*, 2020, **585**, 518–523.
43 J. U. Woo, H. G. Hwang, S. M. Park, T. G. Lee and S. Nahm, *Appl. Mater. Today*, 2020, **19**, 100582.
44 S. R. Zhang, L. Zhou, J. Y. Mao, Y. Ren, J. Q. Yang, G. H. Yang, X. Zhu, S. T. Han, V. A. L. Roy and Y. Zhou, *Adv. Mater. Technol.*, 2019, **4**, 1800342.
45 I. T. Wang, C. C. Chang, L. W. Chiu, T. Chou and T. H. Hou, *Nanotechnology*, 2016, **27**, 365204.
46 X. Yan, L. Zhang, H. Chen, X. Li, J. Wang, Q. Liu, C. Lu, J. Chen, H. Wu and P. Zhou, *Adv. Funct. Mater.*, 2018, **28**, 1–10.
47 X. Zhang, W. Wang, Q. Liu, X. Zhao, J. Wei, R. Cao, Z. Yao, X. Zhu, F. Zhang, H. Lv, S. Long and M. Liu, *IEEE Electron Device Lett.*, 2018, **39**, 308–311.
48 H. Kalita, A. Krishnaprasad, N. Choudhary, S. Das, D. Dev, Y. Ding, L. Tetard, H. S. Chung, Y. Jung and T. Roy, *Sci. Rep.*, 2019, **9**, 1–8.
49 P. Stoliar, J. Tranchant, B. Corraze, E. Janod, M. P. Besland, F. Tesler, M. Rozenberg and L. Cario, *Adv. Funct. Mater.*, 2017, 27.
50 X. Zhang, J. Lu, Z. Wang, R. Wang, J. Wei, T. Shi, C. Dou, Z. Wu, J. Zhu, D. Shang, G. Xing, M. Chan, Q. Liu and M. Liu, *Sci. Bull.*, 2021, **66**, 1624–1633.
51 C. Yoon, G. Oh and B. H. Park, *Nanomaterials*, 2022, **12**, 1728.
52 C. Wan, P. Cai, M. Wang, Y. Qian, W. Huang and X. Chen, *Adv. Mater.*, 2020, **32**, 1902434.
53 J. Y. Kwon, J. E. Kim, J. S. Kim, S. Y. Chun, K. Soh and J. H. Yoon, *Exploration*, 2024, **4**, 20220162.
54 A. D. Craig, *Nat. Rev. Neurosci.*, 2002, **3**, 655–666.
55 S. Cohen and M. E. Greenberg, *Annu. Rev. Cell Dev. Biol.*, 2008, **24**, 183–209.
56 Y. H. Jung, B. Park, J. U. Kim and T. I. Kim, *Adv. Mater.*, 2019, **31**, 1803637.
57 J. Sandkuhler, *Physiol. Rev.*, 2009, **89**, 707–758.
58 R. Wang, J.-Q. Yang, J.-Y. Mao, Z.-P. Wang, S. Wu, M. Zhou, T. Chen, Y. Zhou and S.-T. Han, *Adv. Intell. Syst.*, 2020, **2**, 2000055.
59 G. Zhou, Z. Wang, B. Sun, F. Zhou, L. Sun, H. Zhao, X. Hu, X. Peng, J. Yan, H. Wang, W. Wang, J. Li, B. Yan, D. Kuang, Y. Wang, L. Wang and S. Duan, *Adv. Electron. Mater.*, 2022, **8**, 2101127.
60 T. Moon, K. Soh, J. S. Kim, J. E. Kim, S. Y. Chun, K. Cho, J. Yang and J. H. Yoon, *Mater. Horiz.*, 2024, **11**, 4840.
61 A. Vanarse, A. Osseiran and A. Rassau, *Sensors*, 2017, **17**, 2591.
62 J. K. Han, S. Y. Yun, S. W. Lee, J. M. Yu and Y. K. Choi, *Adv. Funct. Mater.*, 2022, **32**, 2204102.
63 X. Zhang, W. Wang, Q. Liu, X. Zhao, J. Wei, R. Cao, Z. Yao, X. Zhu, F. Zhang and H. Lv, *IEEE Electron Device Lett.*, 2017, **39**, 308–311.
64 G. Wei and I. H. Stevenson, *Neural Comput.*, 2021, **33**, 2682–2709.
65 Q. Cheng, S.-H. Song and G. J. Augustine, *Front. Synaptic Neurosci.*, 2018, **10**, 33.
66 H. R. Monday, T. J. Younts and P. E. Castillo, *Annu. Rev. Neurosci.*, 2018, **41**, 299–322.
67 G. Koch, V. Ponzo, F. Di Lorenzo, C. Caltagirone and D. Veniero, *J. Neurosci.*, 2013, **33**, 9725–9733.
68 T. Guo, K. Pan, Y. Jiao, B. Sun, C. Du, J. P. Mills, Z. Chen, X. Zhao, L. Wei, Y. N. Zhou and Y. A. Wu, *Nanoscale Horiz.*, 2022, **7**, 299–310.
69 S. H. Jo and W. Lu, *Nano Lett.*, 2008, **8**, 392–397.
70 S. Chun, J. S. Kim, Y. Yoo, Y. Choi, S. J. Jung, D. Jang, G. Lee, K. I. Song, K. S. Nam, I. Youn, D. Son, C. Pang, Y. Jeong, H. Jung, Y. J. Kim, B. D. Choi, J. Kim, S. P. Kim, W. Park and S. Park, *Nat. Electron.*, 2021, **4**, 429–438.
71 D. Wang, L. Wang, W. Ran, S. Zhao, R. Yin, Y. Yan, K. Jiang, Z. Lou and G. Shen, *Nano Energy*, 2020, **76**, 105109.
72 K. He, Y. Liu, M. Wang, G. Chen, Y. Jiang, J. Yu, C. Wan, D. Qi, M. Xiao, W. R. Leow, H. Yang, M. Antonietti and X. Chen, *Adv. Mater.*, 2020, **32**, 1905399.
73 Y. Lee, J. Park, A. Choe, S. Cho, J. Kim and H. Ko, *Adv. Funct. Mater.*, 2019, **30**, 1904523.
74 D. Dev, M. S. Shawkat, A. Krishnaprasad, Y. Jung and T. Roy, *IEEE Electron Device Lett.*, 2020, **41**, 1440–1443.
75 M. D. Schaffler, L. J. Middleton and I. Abdus-Saboor, *Curr. Psychiatry Rep.*, 2019, **21**, 134.
76 J. H. Yoon, Z. Wang, K. M. Kim, H. Wu, V. Ravichandran, Q. Xia, C. S. Hwang and J. J. Yang, *Nat. Commun.*, 2018, **9**, 417.
77 X. Xu, E. J. Cho, A. A. Talin, E. Lee, A. J. Pascall, M. A. Worsley, J. Zhou, C. C. Cook and J. D. Kuntz, *Adv. Sci.*, 2022, **9**(15), 2200629.
78 Y. G. Song, J. M. Suh, J. Y. Park, J. E. Kim, S. Y. Chun, J. U. Kwon, H. Lee, H. W. Jang, S. Kim, C. Y. Kang and J. H. Yoon, *Adv. Sci.*, 2022, **9**, 1–10.
79 Y. Kim, Y. J. Kwon, D. E. Kwon, K. J. Yoon, J. H. Yoon, S. Yoo, H. J. Kim, T. H. Park, J.-W. Han, K. M. Kim and C. S. Hwang, *Adv. Mater.*, 2018, **30**, 1704320.

80 S. Maksimovic, M. Nakatani, Y. Baba, A. M. Nelson, K. L. Marshall, S. A. Wellnitz, P. Firozi, S.-H. Woo, S. Ranade and A. Patapoutian, *Nature*, 2014, **509**, 617–621.
81 E. L. Graczyk, B. P. Delhaye, M. A. Schiefer, S. J. Bensmaia and D. J. Tyler, *J. Neural Eng.*, 2018, **15**, 046002.
82 C. Wan, G. Chen, Y. Fu, M. Wang, N. Matsuhisa, S. Pan, L. Pan, H. Yang, Q. Wan, L. Zhu and X. Chen, *Adv. Mater.*, 2018, **30**, 18101291.
83 C. Wang, L. Dong, D. Peng and C. Pan, *Adv. Intell. Syst.*, 2019, **1**, 1900090.
84 Y. Lee and J. H. Ahn, *ACS Nano*, 2020, **14**, 1220–1226.
85 M. Wang, J. Tu, Z. Huang, T. Wang, Z. Liu, F. Zhang, W. Li, K. He, L. Pan, X. Zhang, X. Feng, Q. Liu, M. Liu and X. Chen, *Adv. Mater.*, 2022, **34**, 1–8.
86 X. Pan, J. Wang, Z. Deng, Y. Shuai, W. Luo, W. Luo, Q. Xie, Y. Xiao, S. Tang, S. Jiang, C. Wu, F. Zhu, J. Zhang and W. Zhang, *Adv. Intell. Syst.*, 2022, **4**, 2200031.
87 Q. Duan, T. Zhang, C. Liu, R. Yuan, G. Li, P. Jun Tiw, K. Yang, C. Ge, Y. Yang and R. Huang, *Adv. Intell. Syst.*, 2022, **4**, 2200039.
88 H. Kafaligonul, *J. Neuro. Behav. Sci.*, 2014, **1**, 21.
89 D. L. Yamins, H. Hong, C. F. Cadieu, E. A. Solomon, D. Seibert and J. J. DiCarlo, *Proc. Natl. Acad. Sci. U. S. A.*, 2014, **111**, 8619–8624.
90 Y. Mohsenzadeh, C. Mullin, B. Lahner and A. Oliva, *Sci. Rep.*, 2020, **10**, 4638.
91 M. H. Herzog and A. M. Clarke, *Front. Comput. Neurosci.*, 2014, **8**, 135.
92 G. R. Yang and X. J. Wang, Artificial neural networks for neuroscientists: a primer, *Neuron*, 2020, **107**(6), 1048–1070.
93 B. Dang, K. Liu, X. Wu, Z. Yang, L. Xu, Y. Yang and R. Huang, *Adv. Mater.*, 2023, **35**, 2204844.
94 X. Shan, C. Zhao, X. Wang, Z. Wang, S. Fu, Y. Lin, T. Zeng, X. Zhao, H. Xu, X. Zhang and Y. Liu, *Adv. Sci.*, 2022, **9**, 2104632.
95 Y. Xu, S. Gao, Z. Li, R. Yang and X. Miao, *Adv. Intell. Syst.*, 2022, **4**, 2200210.
96 Y. Pei, Z. Li, B. Li, Y. Zhao, H. He, L. Yan, X. Li, J. Wang, Z. Zhao, Y. Sun, Z. Zhou, J. Zhao, R. Guo, J. Chen and X. Yan, *Adv. Funct. Mater.*, 2022, **32**, 2203454.
97 Y. Wang, Y. Gong, S. Huang, X. Xing, Z. Lv, J. Wang, J. Q. Yang, G. Zhang, Y. Zhou and S. T. Han, *Nat. Commun.*, 2021, **12**, 5979.
98 J. Li, Y. Zhou, Y. Li, C. Yan, X.-G. Zhao, W. Xin, X. Xie, W. Liu, H. Xu and Y. Liu, *ACS Photonics*, 2024, **11**, 4578–4587.
99 L. Ng, M. W. Kelley and D. Forrest, *Nat. Rev. Endocrinol.*, 2013, **9**, 296–307.
100 J. H. Lee, M. Y. Lee, Y. Lim, J. Knowles and H. W. Kim, *J. Tissue Eng.*, 2018, **9**, 2041731418808455.
101 M. Cortada, S. Levano and D. Bodmer, *Int. J. Mol. Sci.*, 2021, **22**, 6368.
102 L. Sun, Y. Zhang, G. Hwang, J. Jiang, D. Kim, Y. A. Eshete, R. Zhao and H. Yang, *Nano Lett.*, 2018, **18**, 3229–3234.
103 B. Gao, Y. Zhou, Q. Zhang, S. Zhang, P. Yao, Y. Xi, Q. Liu, M. Zhao, W. Zhang, Z. Liu, X. Li, J. Tang, H. Qian and H. Wu, *Nat. Commun.*, 2022, **13**, 2026.
104 F. Moro, E. Hardy, B. Fain, T. Dalgaty, P. Clémençon, A. De Prà, E. Esmanhotto, N. Castellani, F. Blard, F. Gardien, T. Mesquida, F. Rummens, D. Esseni, J. Casas, G. Indiveri, M. Payvand and E. Vianello, *Nat. Commun.*, 2022, **13**, 3506.
105 L. Cheng, L. Gao, X. Zhang, Z. Wu, J. Zhu, Z. Yu, Y. Yang, Y. Ding, C. Li, F. Zhu, G. Wu, K. Zhou, M. Wang, T. Shi and Q. Liu, *Front. Neurosci.*, 2022, **16**, 982850.
106 S. Seo, B. S. Kang, J. J. Lee, H. J. Ryu, S. Kim, H. Kim, S. Oh, J. Shim, K. Heo, S. Oh and J. H. Park, *Nat. Commun.*, 2020, **11**, 3936.
107 X. Wu, B. Dang, H. Wu, X. Dalgaty and P. Yang, *Adv. Intell. Syst.*, 2022, **4**, 2100151.
108 A. Rinaldi, *EMBO Rep.*, 2007, **8**, 629–633.
109 K. E. Whitlock and M. F. Palominos, *Front. Neuroanat.*, 2022, **16**, 831602.
110 C. Huart, P. Rombaux and T. Hummel, *Molecules*, 2013, **18**, 11586–11600.
111 G. M. Shepherd, *Nature*, 2006, **444**, 316–321.
112 A. L. Saive, J. P. Royet and J. Plailly, *Front. Behav. Neurosci.*, 2014, **8**, 240.
113 Q. Lu, F. Sun, Y. Dai, Y. Wang, L. Liu, Z. Wang, S. Wang and T. Zhang, *Nano Res.*, 2021, **15**, 423–428.
114 T. Wang, X.-X. Wang, J. Wen, Z.-Y. Shao, H.-M. Huang and X. Guo, *Adv. Intell. Syst.*, 2022, **4**, 2200047.
115 J.-K. Han, M. Kang, J. Jeong, I. Cho, J.-M. Yu, K.-J. Yoon, I. Park and Y.-K. Choi, *Adv. Sci.*, 2022, **9**, 2106017.
116 S. Y. Chun, Y. G. Song, J. E. Kim, J. U. Kwon, K. Soh, J. Y. Kwon, C.-Y. Kang and J. H. Yoon, *Adv. Mater.*, 2023, **35**, 2302219.
117 D. Lee, M. J. Yun, K. H. Kim, S. Kim and H.-D. Kim, *ACS Sens.*, 2021, **6**, 4217–4224.
118 C. Ban, X. Min, J. Xu, F. Xiu, Y. Nie, Y. Hu, H. Zhang, M. Eginligil, J. Liu, W. Zhang and W. Huang, *Adv. Mater. Technol.*, 2021, **6**, 2100366.
119 Z. Gao, S. Chen, R. Li, Z. Lou, W. Han, K. Jiang, F. Qu and G. Shen, *Nano Energy*, 2021, **86**, 106078.
120 D. Chen, X. Zhi, Y. Xia, S. Li, B. Xi, C. Zhao and X. Wang, *Small*, 2023, **19**, 2301196.
121 L. Wang, P. Zhang, Z. Gao and D. Wen, *Adv. Sci.*, 2024, **11**, 2308610.
122 J. Huang, J. Feng, Z. Chen, Z. Dai, S. Yang, Z. Chen, H. Zhang, Z. Zhou, Z. Zeng and X. Li, *Nano Energy*, 2024, **126**, 109684.
123 L. Xiaoqi, J. Jianbo, L. Guangyu, Z. Bao and Z. Enming, *J. Mater. Sci.:Mater. Electron.*, 2024, **35**, 1608.
124 Z. Lv, S. Zhu, Y. Wang, Y. Ren, M. Luo, H. Wang, G. Zhang, Y. Zhai, S. Zhao, Y. Zhou, M. Jiang, Y.-B. Leng and S.-T. Han, *Adv. Mater.*, 2024, **36**, 2405145.
125 J. Shi, Y. Lin, Z. Wang, X. Shan, Y. Tao, X. Zhao, H. Xu and Y. Liu, *Adv. Mater.*, 2024, **36**, 2314156.
126 Y. Gong, X. Xing, X. Wang, R. Duan, S.-T. Han and B. K. Tay, *Adv. Funct. Mater.*, 2024, **34**, 2406547.
127 X. Wang, C. Chen, L. Zhu, K. Shi, B. Peng, Y. Zhu, H. Mao, H. Long, S. Ke, C. Fu, Y. Zhu, C. Wan and Q. Wan, *Nat. Commun.*, 2023, **14**, 3444.
128 J. Lee, B. H. Jeong, E. Kamaraj, D. Kim, H. Kim, S. Park and H. J. Park, *Nat. Commun.*, 2023, **14**, 5775.

129 X. Shan, C. Zhao, X. Wang, Z. Wang, S. Fu, Y. Lin, T. Zeng, X. Zhao, H. Xu, X. Zhang and Y. Liu, *Adv. Sci.*, 2022, **9**, 2104632.
130 J. Yu, F. Zeng, Q. Wan, Z. Lu and F. Pan, *InfoMat*, 2023, **5**, e12458.
131 B. Gao, Y. Zhou, Q. Zhang, S. Zhang, P. Yao, Y. Xi, Q. Liu, M. Zhao, W. Zhang, Z. Liu, X. Li, J. Tang, H. Qian and H. Wu, *Nat. Commun.*, 2022, **13**, 2026.
132 F. Moro, E. Hardy, B. Fain, T. Dalgaty, P. Clémençon, A. De Prà, E. Esmanhotto, N. Castellani, F. Blard, F. Gardien, T. Mesquida, F. Rummens, D. Esseni, J. Casas, G. Indiveri, M. Payvand and E. Vianello, *Nat. Commun.*, 2022, **13**, 3506.
133 C. Sbandati, S. Stathopoulos, P. Foster, N. D. Peer, C. Sestito, A. Serb, S. Vassanelli, D. Cohen and T. Prodromakis, *Sci. Adv.*, 2024, **10**, eadp7613.
134 R. Chaurasiya, K.-T. Chen, L.-C. Shih, Y.-C. Huang and J. S. Chen, *Adv. Theory Simul.*, 2024, **7**, 2301074.
135 L. Wang, W. Li, L. Wan and D. Wen, *ACS Sens.*, 2023, **8**, 4810–4817.
136 T. Wang, H.-M. Huang, X.-X. Wang and X. Guo, *InfoMat*, 2021, **3**, 804–813.
137 P. Qiu, Y. Qin and Q. Xia, *Sens. Actuators, B*, 2022, **373**, 132730.
138 Y. Yoon, Y. Kim, W. S. Hwang and M. Shin, *Adv. Electron. Mater.*, 2023, **9**, 2300098.
139 Y. Qin, M. Wu, N. Yu, Z. Chen, J. Yuan and J. Wang, *ACS Appl. Electron. Mater.*, 2024, **6**, 4939–4947.
140 J.-K. Han, M. Seo, W.-K. Kim, M.-S. Kim, S.-Y. Kim, M.-S. Kim, G.-J. Yun, G.-B. Lee, J.-M. Yu and Y.-K. Choi, *IEEE Electron Device Lett.*, 2019, **41**, 208–211.
141 J.-K. Han, J. Oh, G.-J. Yun, D. Yoo, M.-S. Kim, J.-M. Yu, S.-Y. Choi and Y.-K. Choi, *Sci. Adv.*, 2021, **7**, eabg8836.
142 L. Wang, L. Zhang, S. Hua, Q. Fu and X. Guo, *Sci. China Mater.*, 2025, 1–8.
143 S. Seo, B. Kim, D. Kim, S. Park, T. R. Kim, J. Park, H. Jeong, S.-O. Park, T. Park and H. Shin, *Nat. Commun.*, 2022, **13**, 6431.
144 J. Park, Y. Jang, J. Lee, S. An, J. Mok and S. Y. Lee, *Adv. Electron. Mater.*, 2023, **9**, 2201306.
145 X. Yan, Q. Zhao, A. P. Chen, J. Zhao, Z. Zhou, J. Wang, H. Wang, L. Zhang, X. Li and Z. Xiao, *Small*, 2019, **15**, 1901423.
146 J. Bera, A. Betal, A. Sharma, U. Shankar, A. K. Rath and S. Sahu, *ACS Appl. Nano Mater.*, 2022, **5**, 8502–8510.
147 A. Betal, J. Bera, A. Sharma, A. K. Rath and S. Sahu, *Phys. Chem. Chem. Phys.*, 2023, **25**, 3737–3744.

